Baseline maps of U.S. mature and old-growth forests for conservation and management

ENVIRONMENTAL RESEARCH
ECOLOGY

OPEN ACCESS

RECEIVED
7 November 2025

REVISED
4 March 2026

ACCEPTED FOR PUBLICATION
17 March 2026

PUBLISHED
27 March 2026

PAPER

Baseline maps of U.S. mature and old-growth forests for conservation and management

Jamis M Bruening[1,*], Paul B May[2,3], Ralph O Dubayah[1], Luke Wertis[1], Colin Quinn[4,5], Neil Pederson[6,7], Amanda H Armstrong[4,5] and Ben Poulter[4,8]

[1] Department of Geographical Sciences, University of Maryland, College Park, MD 20742, United States of America
[2] Department of Mathematics, South Dakota School of Mines & Technology, Rapid City, SD 57701, United States of America
[3] Department of Electrical Engineering & Computer Science, Rapid City, SD 57701, United States of America
[4] NASA Goddard Space Flight Center, Greenbelt, MD 20771, United States of America
[5] Earth System Science Interdisciplinary Center, College Park, MD 20740, United States of America
[6] Harvard Forest, Harvard University, Petersham, MA 01366, United States of America
[7] Independent Scholar, Maynard, MA 01754, United States of America
[8] Spark Climate Solutions, Covina, CA 91723, United States of America
[*] Author to whom any correspondence should be addressed.

E-mail: jamis@umd.edu

Keywords: old-growth, enhanced forest inventory, remote sensing, forest structure, Bayesian inference

Supplementary material for this article is available online

Abstract

Mature and old-growth (MOG) forests hold significant ecological and societal value in the United States. In 2022, a presidential executive order directed the U.S. Forest Service to conduct a MOG forest inventory, and regional definitions were developed using the Forest Inventory and Analysis (FIA) system. However, the sparse forest inventory network limited estimates to coarse area-level summaries, and efforts to include specific MOG forest management practices in National Forest management plans were abandoned. National-scale MOG forest mapping at high spatial resolution is essential for balancing and harmonizing MOG conservation, stewardship and management directives, and several recent studies have produced such maps. These approaches either apply alternative definitions, interpolate MOG information without incorporating empirical data at prediction locations, or define MOG characteristics from remote sensing products rather than inventory data. Thus, an enhanced MOG forest inventory that leverages both the national FIA MOG classifications and empirical remote sensing data for predictions remains a pressing need. Here, we developed a spatial Bayesian modeling framework that uses remotely sensed predictor variables to operationalize the FIA plot-level MOG definitions into spatially continuous, fine-scale inference across the conterminous U.S. Our models produce posterior distributions of MOG class presence at 1 ha resolution, enabling probability surfaces and aggregated estimates with transparent uncertainty at policy and ecologically relevant scales. Cross-validation revealed minimal bias nationally but moderate over-prediction in some strata. We estimate that, on all lands, 154.83 million ha contain mature forest and 25.17 million ha contain old-growth—respectively 43.74% and 8.57% of forest area. Our work advances spatial modeling techniques for integrating inventory plot and remote sensing data to characterize complex, context-dependent forest attributes consistently across large geographic extents. This study produces publicly available, spatially continuous MOG information based on the national definitions, providing a foundational resource to inform MOG forest management and conservation.

1. Introduction

Enduring, ancient forest ecosystems are among the most ecologically significant landscapes on Earth (Wirth *et al* 2009a). For millennia, Indigenous communities throughout the present-day coterminous

United States (CONUS) coexisted with forested landscapes, practicing ecological stewardship that helped shape forest structure and composition (White *et al* 2011, Taylor *et al* 2016, Roos *et al* 2021, Tulowiecki 2024). In contrast, increased population densities and technological advances of the industrial revolution brought widespread forest degradation and deforestation that profoundly altered forest landscapes over the past five centuries (Davis 1996). Today, forests that escaped intense anthropogenic disturbance are rare and highly fragmented. Some have been labeled as 'old-growth'—an imprecise yet restrictive term with varied definitions, generally encompassing forests with old trees and characteristics that develop over a long time in the absence of human-induced disturbance (Wirth *et al* 2009b). 'Mature' forest is a less restrictive term, perhaps more related to management than old-growth but with similar ambiguity, and often refers to the stage of stand development after the culmination of mean annual increment, when a slow progression toward old-growth status initiates as gap-scale processes take over and landscape complexity develops (Molina-Valero *et al* 2021, Barnett *et al* 2023, Frye *et al* 2025).

Mature and old-growth (MOG) forests contain immense ecological, cultural, and commercial value. Together, these forests have attracted considerable interest from scientific institutions, conservation groups, the commercial logging industry, federal and Tribal governments, outdoor recreationists, and naturalists (Owen *et al* 2009, Moore and Nelson 2023). Given the diversity of viewpoints and agendas among MOG stakeholders, the challenge of defining, locating, managing, and protecting MOG forests in a manner satisfactory to all is inherently complex and impossible to fully resolve, due to competing priorities and the intersection of science, values, and policy (Pesklevits *et al* 2011, Gray *et al* 2023). In recent decades, several efforts have aimed to systematically define MOG forests in the U.S. (Various authors 1993, Gaines *et al* 1997, Tyrrell 1998). However, a nationally coordinated approach to define and inventory MOG forests was not completed until 2023 (Barndt *et al* 2023). This effort was undertaken in response to Executive Order 14 072, which directed the U.S. Forest Service (USFS) and Bureau of Land Management (BLM) to collaboratively develop definitions for MOG forests, conduct an inventory of such forests on federally owned lands, and release the results publicly (Executive Order 14072 2022).

To fulfill this mandate, definitions of MOG forests were developed for the U.S. Forest Inventory and Analysis (FIA) plot system. Unique definitions of MOG forest classes were independently created for each FIA region, with criteria based on a suite of stand-level inventory variables measured on FIA plots (Pelz *et al* 2023, Woodall *et al* 2023). For all major forest types in a region, a threshold value was established for each variable to collectively identify the onset of MOG characteristics; stands whose metrics exceeded all thresholds were classified accordingly. These regional, forest type- and class-specific definitions were applied to all FIA plots located in U.S. National Forests or BLM-owned lands, resulting in stand-level forest classifications of old-growth, mature, or neither that served as the basis for the national MOG inventory. In this paper, we refer to these definitions as 'the national definitions,' and our goal is to produce CONUS-wide, spatially explicit maps of MOG forests based on these definitions.

Implicit in the national definitions is an assumption rooted in traditional models of stand development—that structural attributes serve as reliable proxies for tree age and forest history (e.g. Oliver *et al* 1996). The MOG definitions across all regions rely primarily on structural criteria, in that biophysical attributes (e.g. tree diameters, stand basal area) were given equal or greater weight in defining MOG classes than age-related criteria (e.g. individual ages or stand age structure; see the supplementary note). Therefore, the nationally defined MOG classes represent forests with nuanced structural and temporal characteristics, derived from decades of forest ecology research across all major U.S. forest types, and must not be interpreted as forest age classes. The old-growth definitions (see Pelz *et al* 2023) require a distinct and selective set of criteria to be met for each FIA region, while the mature criteria (see Woodall *et al* 2023) are a relaxed and standardized version of each regional old-growth definition, allowing for a more diverse set of mature class realizations.

The FIA program maintains a network of plots throughout CONUS, the locations of which are determined through a quasi-systematic sample design that is assumed to well approximate a simple random sample of the landscape. Forest characteristics are sampled on plots where the land cover meets the FIA definition of forest, enabling design-based estimates of forest attributes across geographic areas with an adequate sample size (Bechtold and Patterson 2005). In this way, the national MOG inventory produced acreage estimates for MOG forest classes on federal land within a coarse polygon grid. Precise locations of MOG forests were masked by a spatial estimation unit of approximately 1000 km^2 (Ager *et al* 2021, Barndt *et al* 2023), and a subsequent effort to incorporate MOG-specific management actions in U.S. National Forest management plans did not proceed to implementation (Chief Randy Moore 2025).

Several recent mapping studies have applied different methodologies for continuous, high-resolution MOG inference across CONUS; two are enhanced forest inventory techniques that leverage FIA data in both the definition and mapping framework and a third uses remotely sensed information to define and map MOG forests. Barnett *et al* (2023) derived forest type-specific 'functional' MOG definitions from

biomass-accumulation curves fit from FIA inventory data, and used plot imputation techniques to produce a continuous MOG classification surface at 30 m spatial resolution. Herrera *et al* (2025) applied the national MOG definitions to FIA plots, generated an 'old-growthness' index from the MOG classifications, and interpolated this index across CONUS forested lands at locations not sampled by the FIA program. They identified forested pixels eligible for prediction using a remotely sensed canopy cover map, and interpolated the index into forested pixels using inverse distance weighting of the index values from the nearest three FIA plots. In contrast, DellaSala *et al* (2022) produced a national relative maturity map by assigning regional quartiles for canopy height, biomass, and canopy cover layers derived from remote sensing data, summing those quartile scores to form an ordinal 0–9 index and then classifying pixels into a set of successional classes. Together these studies demonstrate useful and complementary ways to map MOG-related information. However, the inventory-based approaches rely on imputed stand attributes or spatial interpolation of plot-derived indices for mapping, such that predictions at unsampled locations are not informed by direct observation, nor is uncertainty in class membership acknowledged or propagated. Remote sensing-only approaches indirectly define MOG characteristics from remote sensing data products rather than observed forest inventory criteria, and therefore represent generalized relative structure rankings rather than nuanced and precise biophysical classifications. Collectively, these works highlight both a growing appetite for enhanced forest inventory methods of MOG prediction informed by the FIA plots and empirical observation, and the challenges associated with generating this information accurately and consistently across large areas.

Forest management priorities of the current U.S. administration elevate the role of sustainable commercial timber harvest and wildfire risk mitigation (Executive Order 14223 2025, Executive Order 14225 2025) and amplify the need for spatially explicit, empirically grounded inference into forest structure and successional classes across CONUS. Informing forest management decisions with science-based spatial data and methods will help satisfy national priorities while also supporting environmental stewardship and conservation. This underscores the urgent need for spatially precise, wall-to-wall baseline maps of MOG forests grounded in empirical observation, not only to support durable protections for remaining old-growth landscapes but also to provide scientific information to guide adaptive managers supporting national forest policy. Accordingly, two pressing scientific questions must be addressed: How much MOG forest exists throughout CONUS, and where is it located? Our paper aims to support both old-growth stewardship and national forest management priorities by producing high-resolution, spatially continuous MOG forest maps.

We address these science questions by shifting estimation paradigms from a design-based approach reliant on the national forest inventory, to a model-based approach that harmonizes the plot-level MOG classifications with remote sensing data for spatially continuous inference. Definitive, continental-scale MOG maps are precluded both by the diversity of definitions in scientific literature (Hilbert and Wiensczyk 2007) and by the myriad ways to link sparsely sampled forest inventories with remote sensing (e.g. Duncanson *et al* 2022, Bruening *et al* 2023, May *et al* 2024). Therefore, our work represents one of many possible interpretations of forest structure dynamics at this current snapshot in time, in the context of MOG forests as defined by the U.S. government. We developed a Bayesian spatial modeling framework for wall-to-wall regional MOG classification, using data from spaceborne missions—the Global Ecosystem Dynamics Investigation (GEDI), Landsat 8, Sentinel-2, ALOS PALSAR-2, and Shuttle Radar Topography space missions (Hansen *et al* 2013, JPL 2013, JAXA 2018, Friedl 2020, Dubayah *et al* 2021, Lang *et al* 2023, May *et al* 2024)—in a quadratic discriminant analysis (QDA) informed by the national definitions. In model training, we spatially joined FIA plot-level MOG classifications with remote sensing predictors to characterize an empirical multi-dimensional signature of remotely sensed information associated with each MOG class. The QDA models were then applied to the stack of predictors to generate a posterior distribution of class occurrence for each land pixel in a 1 ha resolution grid covering CONUS, comprised of the following mutually exclusive classes: non-forest, old-growth forest, mature forest, and other forest. The posterior class distributions were then used to generate two map types that enable broad-scale MOG reporting and localized forest management and conservation activities:

1. separate probability surfaces of MOG class occurrence at 1 ha spatial resolution, and
2. separate estimates of MOG forest area and proportion, with transparent uncertainty, at national, regional, and 25 km^2 (5 km $\times$ 5 km) spatial resolutions.

This analysis is not an exercise in forest age modeling or mapping. The national MOG definitions are based on decades of ecological research, and delineate specific classes related to forest structure and

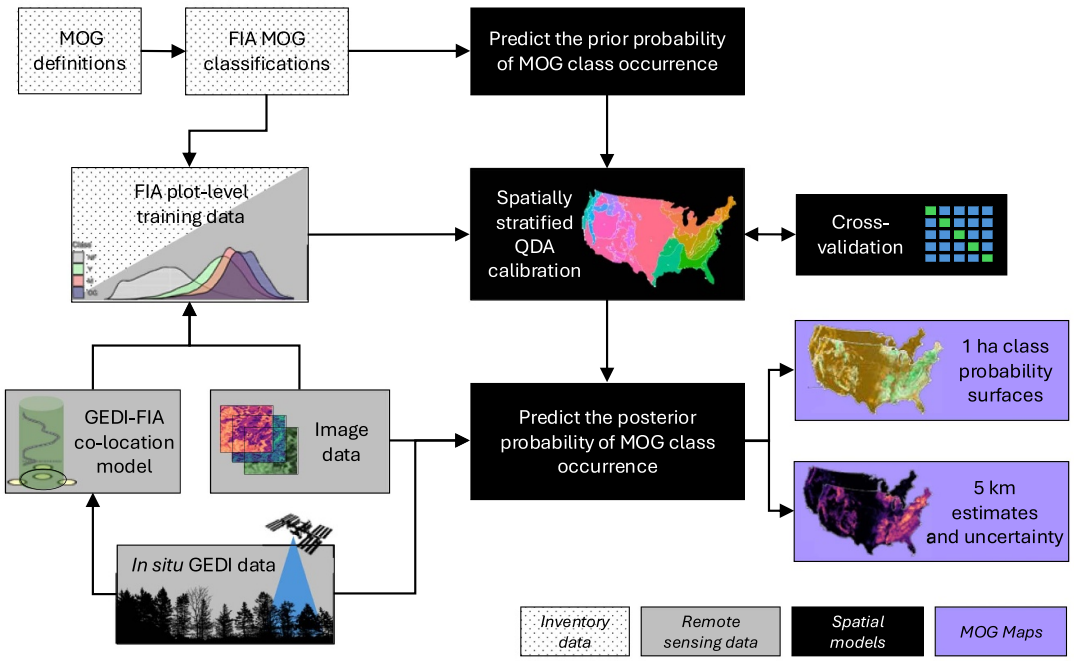

Figure 1. Methods overview. MOG definitions were applied to FIA plots, which were spatially intersected with the remote sensing predictor variables to build our model training data. The training data were segmented into 29 strata, and individual forest, mature and old-growth QDA models were calibrated for each. FIA plot coordinates were also used to generate spatial prior probability surfaces. The models were then applied to generate posterior distributions of class occurrence, informed by the prior probabilities and *in situ* remote sensing data. From the posterior distributions we generated 1 ha class probability surfaces and area-level class proportion estimates.

life-history that go far beyond mean forest age mapping. Because MOG ecosystems are of high ecological and management importance, we emphasize mapped MOG information be grounded in direct observations, ensuring that high-stakes decisions are informed by empirical evidence rather than exclusively interpolated or imputed information. Our work simply provides probabilistic inference into the presence of these MOG classes everywhere on the CONUS landscape, derived from an initial prior probability that is subsequently updated at every prediction location, based on empirically derived remote sensing products that are highly related to the definition criteria. We discovered previously unknown spatial patterns in MOG forest distribution and produced statistically rigorous national and regional estimates with uncertainty. We present our maps as a benchmark for monitoring changes in the distribution of MOG forests across CONUS and informing MOG forest stewardship and management.

2. Methods

Our analysis (figure 1) integrates plot-level MOG forest classifications derived from U.S. FIA data with remotely sensed predictors to produce spatially explicit maps of forest, mature, and old-growth occurrence probability across the CONUS. We converted FIA stand-level MOG definitions into categorical response variables and joined the plot data with a suite of remote sensing variables to construct model training data. The plot labels and remote sensing predictors were used to calibrate spatially explicit quadratic discriminant classifiers, from which we produced posterior class probabilities at 1 ha resolution and area-level estimates with uncertainty. The components of this workflow are described below and in appendix.

2.1. Forest inventory MOG classifications

The national MOG definitions were used to classify forest stands on FIA plots as mature, old-growth, or neither (see Pelz *et al* 2023, Woodall *et al* 2023). The MOG definition criteria varied by administrative region (table 1 and figure 2). In regions 1–6 some FIA tree-level information required by the definitions was not publicly available, and as a result, we could not reproduce the MOG classifications ourselves in those regions. Instead, we used the MOG classifications from Woodall *et al* (2023) for all forested plots

Table 1. FIA tree- and stand-level attributes used in old-growth definition criteria across regions. Only the tree- and stand-age variables contain information directly related to time. The other attributes contain physical information that reflects tree- and stand-structure. Region 6a refers to the Northwest Forest Plan (NWFP) area and 6b refers to land in region 6 outside the NWFP. DBH stands for Diameter at Breast Height. Other includes Zeide's Stand Density Index, Quadratic Mean Diameter, and the Diameter Diversity Score.

	Tree-level attributes						Stand-level attributes		
Region	Large tree DBH	Large tree age	Large tree density	Damaged tree density	Snag DBH	Snag density	Basal area	Stand age	Other
1	x	x	x				x		
2	x	x	x	x		x			
3	x								x
4	x	x	x						
5	x		x					x	
6a	x		x		x	x			x
6b	x		x					x	
8	x					x	x	x	
9	x	x						x	

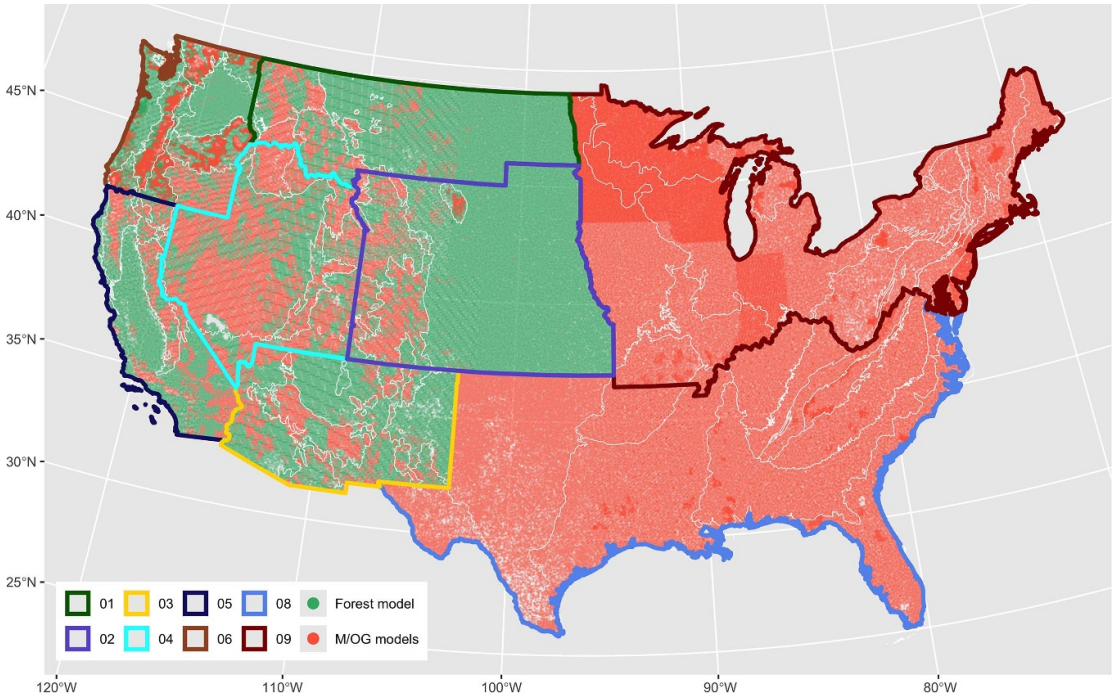

Figure 2. FIA regions (colored lines) and all CONUS FIA plots used to calibrate the QDA models. Red points represent plots used for all class models (forest, mature, and old-growth) while green points represent FIA plots used only for the forest models in a given strata. This distinction is necessary, because in regions 01–06, we did not have access to MOG classifications on FIA plots outside public lands (green points). These FIA plots were thus only used for the forest model, and excluded from the mature and old-growth models (red points).

on USFS and BLM lands. In regions 8 and 9 the necessary FIA data were available, and we applied the MOG definitions to the FIA inventory data for all plots from the most recent inventory cycle.

The MOG definitions are specific to the unit level of FIA sampling—a forest stand. FIA terms these units as 'conditions' which represent clearly delineated, homogeneous areas of forest present in at least one of the four subplots that constitute an FIA plot (Bechtold and Patterson 2005). FIA plots can have a single forest or non-forest condition, or multiple forest or non-forest conditions, and multiple MOG labels can exist within a single FIA plot. We extended the condition-level MOG labels to one of four plot-level labels—non-forest, mature forest, old-growth forest, other forest (forest but neither mature nor old-growth)—according to the following rules: Plots were first classified as forest and eligible for MOG classification if any forest condition was present on the plot. If no forest conditions were present, the plot was classified as non-forest. Considering forest plots, those that contained at least one old-growth

condition were classified as old-growth. Forest plots that did not contain an old-growth condition but did contain a mature condition were classified as mature. Forest plots that did not contain either an old-growth or mature condition were classified as other. The plot-level labels served as the response variable for the QDA models.

2.2. Spatial quadratic discrimination analysis

We mapped all forest, mature forest, and old-growth forest probabilities using a spatially explicit QDA framework, calibrated with FIA plot labels and remotely sensed predictors. A summary of the modeling framework is provided here, with the complete description of the spatial QDA methodology, predictor construction, and model implementation presented in appendix.

To reduce spatial heterogeneity in predictor–response relationships, we segmented CONUS into various strata based on forest composition and U.S. Environmental Protection Agency Level II and III ecoregions, while trying to maintain at least 100 plots in each class within any given stratum. This resulted in 29 unique strata, all with at least 100 mature, other, and non-forest labels (four strata contained slightly fewer than 100 old-growth labels, see table S1). The QDA models were calibrated and applied independently for each stratum. Because the MOG forest classes are hierarchically nested (old-growth $\subset$ mature $\subset$ forest), we implemented a sequence of nested, binary QDA models: 1) forest vs non-forest; 2) MOG combined vs other forest, conditional on forest; and 3) old-growth vs mature, conditional on MOG. Posterior class probabilities were then propagated through stages to obtain class marginal probabilities in each grid cell. Through post-processing this hierarchical formulation yielded mutually exclusive probabilities for four classes: non-forest, other forest, mature forest, and old-growth forest.

We selected a suite of remotely sensed predictor variables representing forest structure, function, and site conditions that were related to the MOG definition criteria. We considered complementary predictor types (see table S2): 1) point-location GEDI waveform metrics describing vertical forest structure within the 25 m diameter lidar footprints, and 2) wall-to-wall gridded remote sensing data representing forest and topographic attributes. The GEDI predictors were imputed waveform metrics at the exact FIA plot locations, representing maximum canopy height and the distribution of vegetation between the ground and top of canopy. Wall-to-wall gridded predictors included multispectral reflectance composites, vegetation phenology timeseries parameters, synthetic aperture radar backscatter, canopy surface texture metrics, a canopy height model, and topographic variables. These data were aggregated from their native spatial resolutions to our 1 ha modeling grid using area-weighted averaging to ensure consistency between predictor support and model resolution. Candidate predictors were evaluated for approximate class-conditional normality, transformed when necessary, centered and scaled, and reduced via a principal components analysis (PCA). We retained the first two principal component projections of the gridded predictors as final QDA model predictors. GEDI waveform metrics were excluded from the PCA for QDA model training to permit downstream prediction in grid cells lacking GEDI observations. QDA models therefore used two PCA components and one GEDI metric when available, and PCA components alone in grid cells not sampled by GEDI.

To address violations of classical QDA assumptions in a spatial context, we extended the framework by modeling both class prior probabilities and class-conditional predictor processes as spatial Gaussian processes with Matérn covariance. Prior probabilities were allowed to vary spatially via a softmax transformation of latent Gaussian fields to ensure valid probability bounds, capturing both large-scale gradients and local clustering in class occurrence. Model parameters were estimated in a Bayesian framework with weakly informative priors, and posterior predictive class probabilities were obtained via Monte Carlo methods.

Area-level totals and proportions were generated by aggregating posterior predictions across grid cells, yielding expected values and 95% credible intervals at national, stratum, and 25 km^2 scales. Model performance was assessed primarily at the unit-level using 10-fold cross-validation within each stratum, with results combined across strata for national scale interpretation, and secondarily at the strata-level through comparisons of design-based area-level estimators using the FIA plot data and our model-based estimates. Final map products were post-processed to report on mutually exclusive mature forest and old-growth forest classes (the supplementary material contains results for an all forest category merging the other, MOG classes).

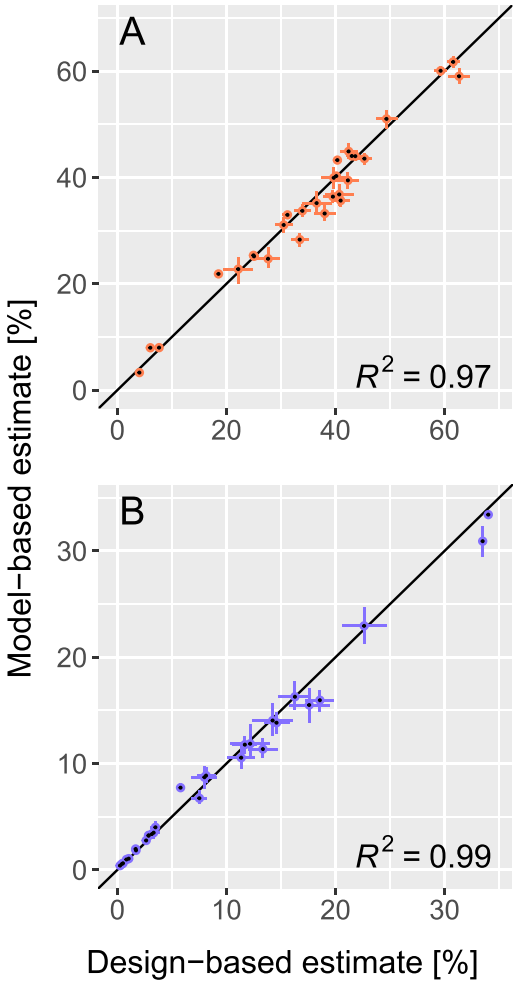

Figure 3. Strata-level comparisons of design-based (produced from the FIA sample) and model-based (predicted) proportion estimates for mature (A) and old-growth (B) forest classes. Each data point represents the estimates for a given strata (from table S3) expressed as a class percentage of total land area. The *x*-axis values and uncertainties are direct estimates and 95% confidence intervals calculated from the FIA plot-level classifications. *Y*-axis values are our model-based estimates with a 95% credible interval.

3. Results

3.1. Area level MOG estimates and uncertainty

We estimated mature forests occur within 154.83 million ha of public and private lands in CONUS, with a 95% credible interval (CI)—defined as the 2.5% and 97.5% quantiles of the posterior probability distribution—of 153.74–155.96 million ha (table S1). Hectares containing mature forest account for 20.09% (CI 19.95%–20.24%) of total land area, and 43.74% (CI 42.48%–44.77%) of forest area. In contrast, we estimated old-growth forests occur within 25.17 (CI 24.47–25.91) million ha, comprising 3.27% (CI 3.18%–3.36%) of total land area and 8.57% (CI 7.87%–9.47%) of forest area (table S1). MOG estimates specific to the modeling stratification (n = 29, figure 9) are reported in table S3. When restricted to the same spatial domain as our FIA training data (figure 2), our strata-level model-based MOG proportion estimates were in agreement with design-based Horvitz–Thompson estimates derived from the FIA plot-level MOG classifications (figure 3). At this spatial scale, our model-based estimates had a slightly higher degree of precision than the design-based estimates (figure S2).

CONUS-wide trends in MOG estimates were evident by longitude (table S3); forests across the entire eastern US (strata 1–13 in figure 9) were predominantly mature with little old-growth. We estimated 60.87% (CI 60.75%–60.99%) of hectares in the eastern U.S. contained forest, 59.34% (CI 58.99%–59.70%) of which contained mature forest, and only 3.23% (CI 3.09%–3.35%) of which contained old-growth. At the strata level, we estimated forests in 11 of the 13 eastern strata were majority mature, although only two strata contained forests with a rate of old-growth occurrence above 5%.

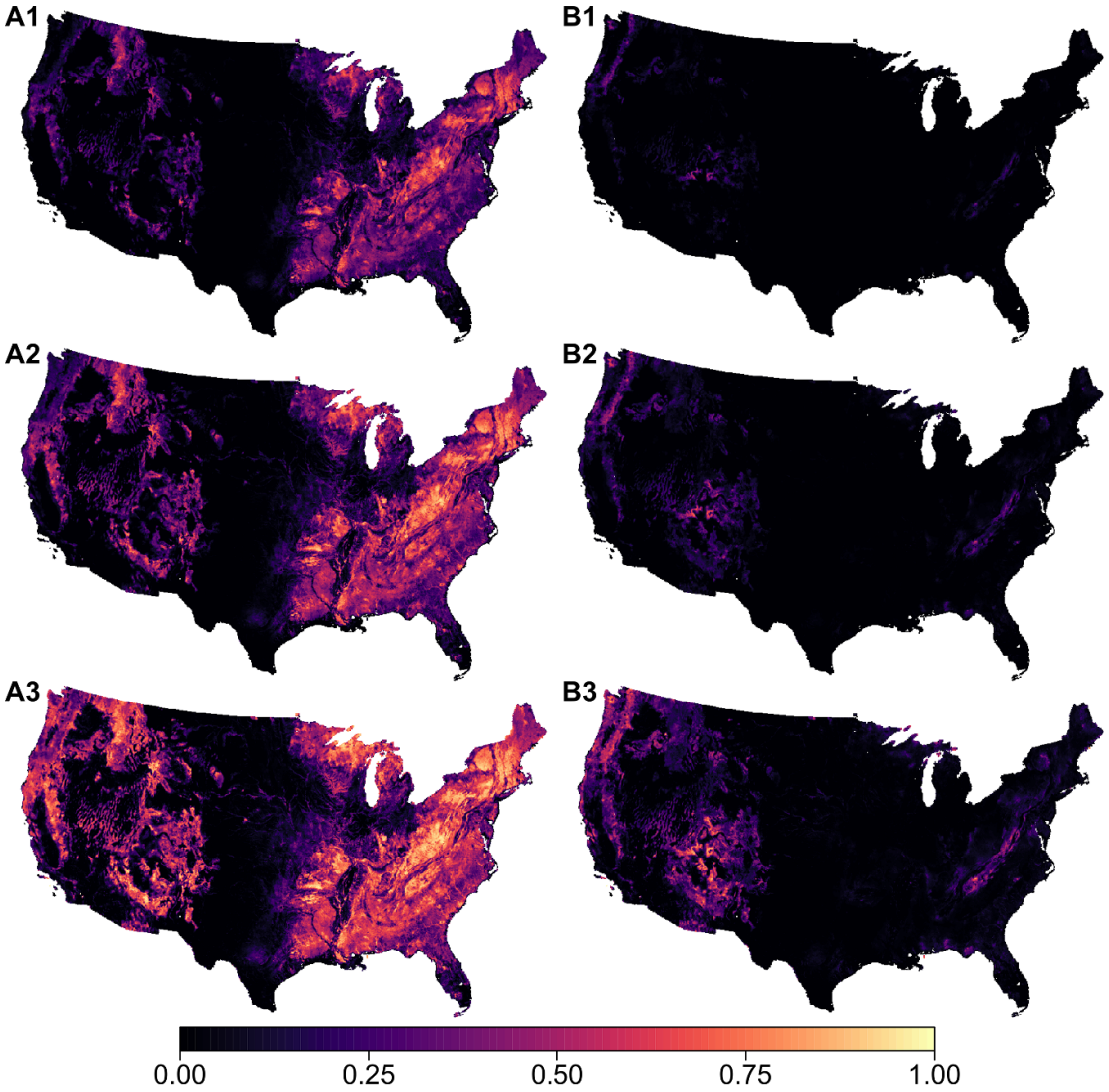

Figure 4. Estimates of mature (A panels) and old-growth (B panels) proportion of total land area, with uncertainty, at 5 km spatial resolution. The expected proportion value for each class is shown in panel 2, with the 2.5% and 97.5% quantiles shown in panels 1 and 3, respectively. All values represent the proportion of hectares within each 5 km pixel that were estimated to contain each class, analogous to the 'total' percentage estimates in table S1.

Forests across the entire coterminous western US (strata 14–28 in figure 9) by contrast contained lower rates of mature forest occurrence than the east, but higher rates of old-growth forest occurrence. Here, 38.96% (CI 38.82%–39.10%) of hectares were estimated to contain forest, of which 33.30% (CI 32.54%–34.04%) and 15.74% (CI 15.09%–16.41%) contained MOG forests, respectively. While no western strata had forests that were a majority mature, all but two contained forests with rates of old-growth occurrence above 10%.

3.2. Spatial patterns of MOG forests

The 1 ha posterior distributions of MOG class occurrence were used to generate two distinct map types of MOG forest classes; 1) 5 km spatial resolution maps (25 km^2) representing the proportion of each pixel's land area occupied by each class and an associated 95% credible interval (figure 4), and 2) 1 ha class occurrence probability surfaces (figure 5 and figure S1). To identify trends within forested areas, we generated histograms of 1 ha MOG occurrence probability (figure 6) from hectare pixels with >50% predicted forest probability (figure S1C). The mature probability within forest pixels tended to be greater and more variable than the old-growth probability, with large regional differences occurring between eastern and western regions.

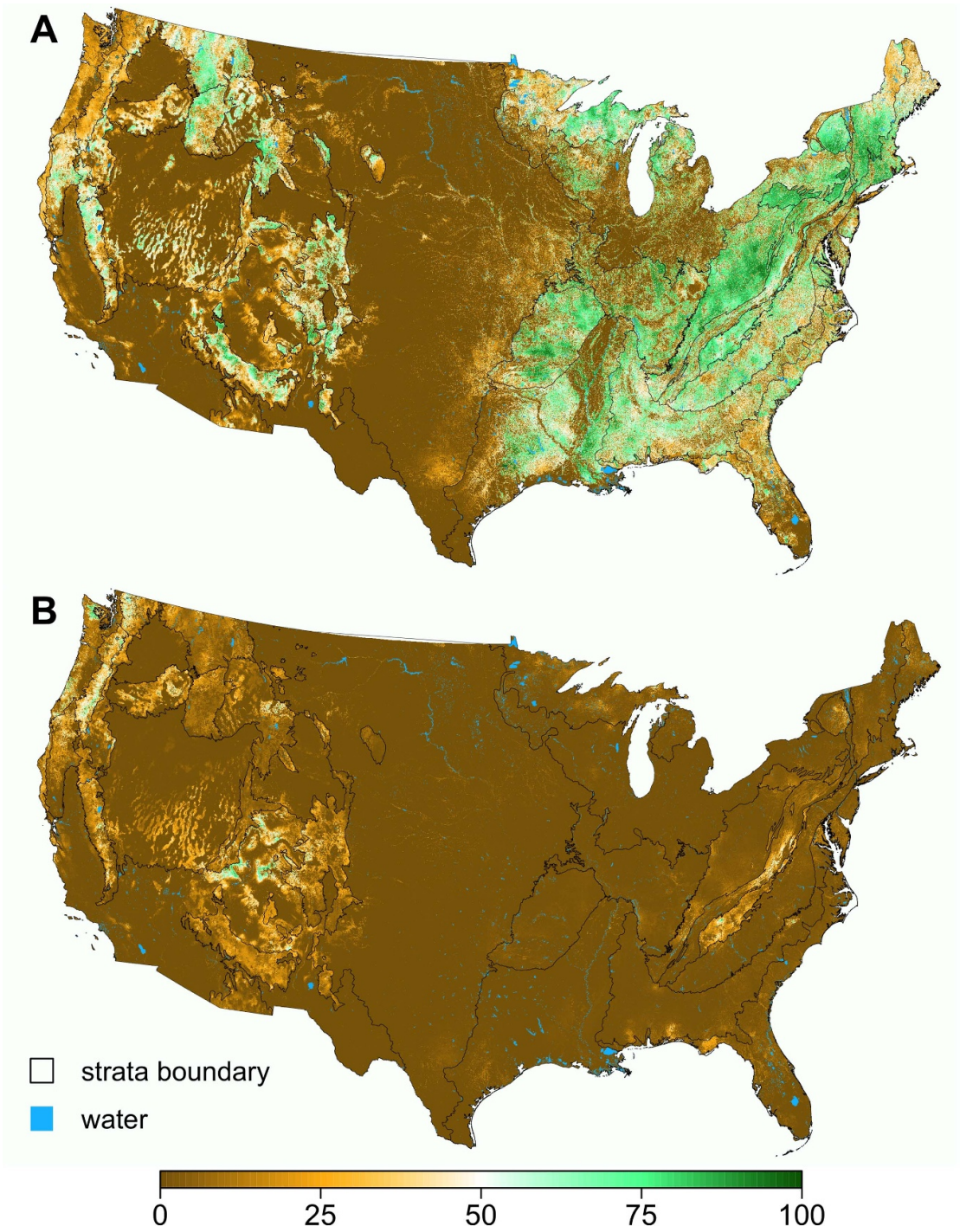

Figure 5. Probability of MOG class occurrence mapped at 1 ha spatial resolution. Mature (A) and old-growth (B) probabilities are shown, with the strata boundaries overlaid in black.

3.3. QDA model cross validation

We define empirical model bias as the difference between the average predicted probability for a given class across a set of observed plot labels, and the proportion of those observed labels in the given class—positive model bias indicates overprediction of posterior probability, and negative model bias indicates underprediction. Cross-validation indicated varying degrees of empirical model bias across the range of predicted MOG probabilities. Collectively, the 29 mature models across CONUS together exhibited slight positive bias (overprediction), with an observed classification rate and average predicted probability of 18.93% and 20.79% respectively. The old-growth models were also positively biased, with a respective observed classification rate and average predicted probability of 2.76% and 3.72%.

Overprediction from positive model bias was primarily concentrated in western strata. Considering western CONUS (strata 14–28), 12.30% of FIA plots were observed as mature, compared to a mean

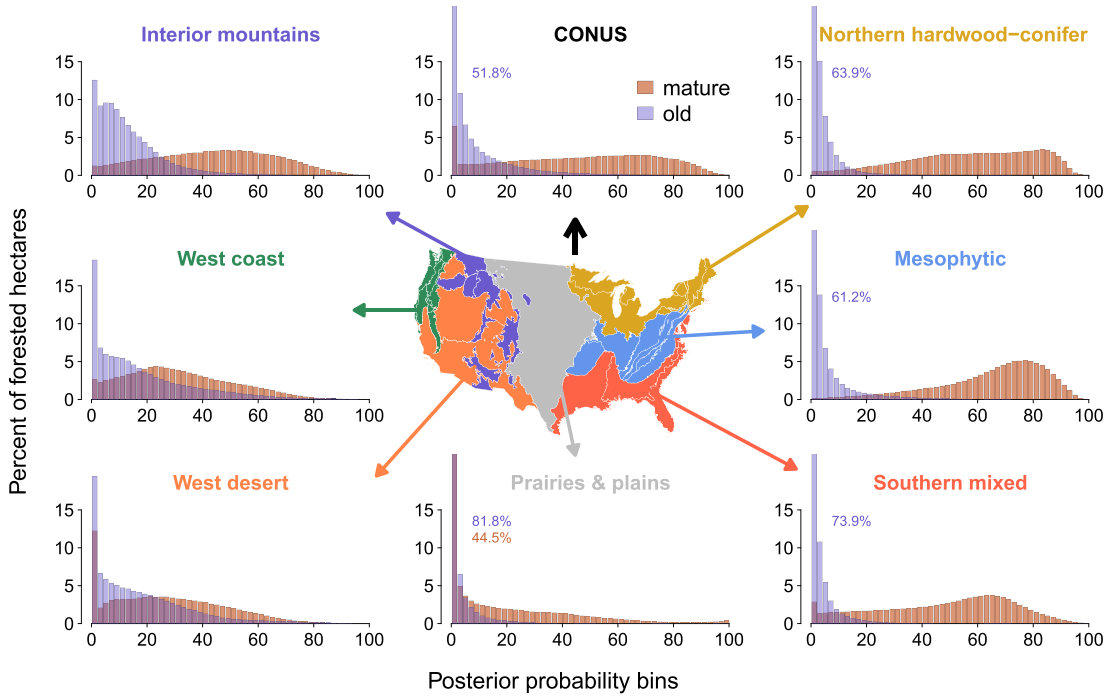

Figure 6. Regional and CONUS-wide distributions of mature and old-growth posterior 1 ha probabilities within forests (hectare pixels with greater than 50% predicted forest probability). The *y*-axes are truncated to show details of the distribution for the larger predicted probabilities, and some plots have percentages in the 0%–2% bin that extend above the top of the *y* axis. These values are printed in the upper left of each plot, colored by class. The inset map shows all 29 strata outlined in white, and the colored regions represent the multiple strata that constitute each regional grouping displayed here.

predicted mature probability of 16.44% across those plots. Respective values for the eastern strata (1–13) were 35.36% and 35.53%. A similar trend was evident in the old-growth models, as 5.70% of FIA plots in the western strata were observed as old-growth, compared to a mean predicted old-growth probability of 8.10% across those plots. In eastern strata, the respective observed fraction and average predicted probability were 2.07% and 2.29%.

The magnitude of empirical model bias varied across the range of predicted probabilities for each class. This was observed when assessing cross-validation results across all 29 strata collectively, and also regionally by eastern (1–13) and western (14–28) strata (figure 7, and figures S4–S8). We evaluated model performance using 10-fold cross validation and merged results from each fold post-hoc for complete assessment of probability calibration across all FIA plots used in model development. FIA plots were grouped into bins (width of 2.5%) based on the predicted class probability at the plot's location. Considering all plots in each 2.5% range of predicted probability, we calculated the observed class proportion (*y*-axis in figure 7), and compared that value to the center of each bin of predicted probabilities (*x*-axis in figure 7).

In a perfectly calibrated model, the observed class proportion equals the center value of the range of predicted probability (i.e. values fall along the black 1:1 line in figure 7). For example, among all FIA plots that received between 80%–82.5% predicted probability of old growth from an unbiased model, approximately 81.25% of those plots would be expected to be old-growth. In figure 7, each bin's vertical bar represents the observed class proportion among held-out FIA plots within a given predicted probability bin across the 10 folds of cross-validation. The difference between the diagonal black 1:1 line and the height of each bar therefore indicates the degree of model bias for that range of predicted probabilities. Bars below the 1:1 line indicate overprediction from positive model bias, meaning the predicted probability exceeds the observed class proportion within that bin, whereas bars above the line indicate underprediction from negative model bias.

Across all strata, the forest models exhibited minor underprediction for probabilities $<50\%$ and minor overprediction for probabilities $>50\%$, both nationally and regionally. In the eastern strata, the mature forest models were well calibrated across the range of predicted probabilities, whereas in the western strata overprediction increased for predicted probabilities $>20\%$. Nationally, the old-growth models exhibited increasing overprediction with increasing predicted old-growth probability, although this trend was stronger in western strata than in eastern strata.

4. Discussion

Our study translates the national MOG definitions to a remote sensing context; we joined forest inventory plot-level MOG classifications with multi-sensor remote sensing data to train spatial QDA classifiers in 29 different ecoregions throughout CONUS. Informed by the prior probability of MOG class occurrence from the FIA plot network and spatially explicit remote sensing data, the models produced a posterior distribution of MOG class occurrence for every land hectare within CONUS. From these posteriors, we 1) estimated MOG total area and proportions with 95% credible intervals at national, ecoregional, and 25 km^2 spatial scales, and 2) mapped the probability of MOG class presence at 1 ha resolution. Our model-based proportion estimates were in agreement with design-based proportion estimates generated from the FIA data used in model training, indicating accuracy in our regional and national estimates. At the hectare scale, cross-validation revealed approximately unbiased models at the strata level, but with localized empirical model biases at finer scales, suggesting over-prediction of MOG occurrence probability that is sparse but spatially clustered.

4.1. Human impacts on MOG forest structures

Regional MOG trends across CONUS (figure 6) coincide with the nation's history of forest disturbance and land use. Differences between Western and Indigenous worldviews underscore the need to distinguish types of human influence on U.S. forests (Eisenberg *et al* 2024). Succession-altering disturbances associated with Euro-American settlement—driven by technological advances and demand for timber and agricultural products—differed from the place-based stewardship practices of Indigenous communities over longer timescales, such as cultural burning and traditional agroecological methods (e.g. Long *et al* 2021, Armstrong *et al* 2022, Tulowiecki 2024). While the full extent of Indigenous stewardship impacts remains an active area of research (Eisenberg *et al* 2019), evidence suggests associated increases in biodiversity, resilience to natural disturbances, and other ecological benefits (Nelson 2012, Lake and Christianson 2020, Hoffman *et al* 2021, Adlam *et al* 2022). Analysis of U.S. old-growth structure must therefore consider the shared history between Indigenous people and forested landscapes, and we acknowledge that current old-growth structure and composition may reflect diverse, place-based stewardship legacies.

Low estimates of old-growth throughout eastern strata (table S3) coincide with Euro-American alteration of forest successional trajectories from harvesting, grazing, and agricultural clearing. Davis (1996) estimated that only 0.52% of eastern forested land was 'known primary forest', suggesting limited destructive anthropogenic activity. This implies either 1) some forest we estimated to be old-growth (3.23% of eastern forests) may have been once disturbed by American settlers, but enough time has passed to allow for old-growth structural conditions to regenerate or 2) Davis's original work underestimated the amount of eastern old-growth. The timing of minimum forest extent in the eastern U.S. varied spatially across the late 19th and early 20th centuries (Davis 1996, Foster and Aber 2004). Subsequent secondary forest regrowth and expansion align with our estimate of majority mature forest (59.34% of forested area), indicating developmental processes have operated long enough for mature structures to proliferate. If mature eastern forests remain undisturbed or guided by active stewardship (e.g. Keeton 2006, Bauhus *et al* 2009, Palik *et al* 2020), a resurgence of old-growth characteristics, under the national definitions, could be achieved.

In western forests, the percent of old-growth forest area was more than five times that of eastern forests (16.74% vs 3.23%), suggesting the spatial extent of intensive anthropogenic disturbance was lower than in the east. However, logging of 'pre-colonial forests' in the west occurred more recently due to later settlement, and recent forest loss from wildfire is greater (Tyukavina *et al* 2022). Less time for regrowth and structural development after stand replacing disturbances aligns with lower mature forest proportion in western forests relative to eastern forests (33.30% vs 56.7%, table S3).

4.2. Importance of MOG definition criteria and inferential methods

The extent to which U.S. forest structures conform to the mature definitions was on average greater than for the old-growth definitions (figure 6). This result highlights a key difference between the classes: the mature definition allows for multiple pathways of structural development into the mature class and thus a greater variety of mature forest structures than the comparatively restrictive old-growth definitions. Our analysis suggests this intent was achieved, with larger magnitudes and greater variability in mature forest probability (figure 6), indicating a more common class and higher diversity of possible mature forest compositions than for old-growth.

The interpretation and utility of MOG maps depend on the underlying definitions. Definition criteria affect estimated MOG extent and spatial patterns (Trouvé *et al* 2023, Bruening *et al* 2024), and contrasting maps understandably raises questions from policy makers and managers and may complicate decision making. This underscores the need to normalize multiple characterizations of old forests, as suggested by Spies (2004). Contrasting our mapping results with similar studies highlights exemplifies this. For example, Barnett *et al* (2023) used the FIA plot network to develop a functional MOG definition to delineate early-seral, young, mature, and old-growth forest classes based on age-related rates of aboveground carbon accumulation. Given the distinct theoretical basis and criteria underlying the national MOG definitions and those of Barnett *et al* (2023), they, unsurprisingly, estimated CONUS forest percentages of MOG (respectively 32.40% and 6.29%) that varied from our estimates (43.74% and 8.57%). Comparing our map (figure 5) with figure 8 in Barnett *et al* (2023) reveals that the degree of similarity between structural and functional MOG characteristics varies spatially. We posit that investigating spatial patterns of convergence and divergence between complementary MOG definitions is perhaps a more useful line of inquiry than reconciling high-level MOG estimate differences, and believe that multiple MOG characterizations provide a more complete and nuanced understanding of old forest characteristics than a single definition.

Future map-harmonization efforts, similar to those for aboveground biomass, would further aid the community (Hunka *et al* 2023, Guala *et al* 2024), and methods should reflect the properties of the constituent maps. For example, Spies and Franklin (1996), presents a landscape-scale definition of old-growth that requires a mosaic of small forest patches in various successional stages, and suggests a minimum of 10 ha to characterize old-growth as a mosaic of one hundred 0.1 ha patches. Integrating an old-growth map based on structural or functional heterogeneity between patches at a coarse scale with a map based on structural or functional homogeneity within a patch when specific thresholds are met as a fine scale (e.g. Barnett *et al* (2023) or our probability surface) would follow a different process than harmonizing maps with more similar definition structures and spatial scales.

In contrast, disagreement in MOG estimates when the same definitions are used instead arise from methodological differences, assuming other potential factors (time period, spatial scale, etc) are negligible. Herrera *et al* (2025) report their interpolation method underpredicts MOG extent by more than 50% relative to the design-based estimates of Pelz *et al* (2023), and Woodall *et al* (2023), when considering the same spatial extent and using the same input inventory data via different inferential frameworks. The Herrera *et al* (2025) approach propagates plot-level MOG information across space by interpolating a continuous index from the three nearest plots via inverse distance weighting, and does not consider empirical structural information at prediction locations. This method will not identify a patch of old-growth in a forest if at least one of the three nearest FIA plots is not also old-growth. The estimate discrepancy may simply be a function of spatial interpolation of a continuous index, which smooths local variation and attenuates extremes through averaging. Subsequent thresholding of the interpolated index may reduce the mapped extent of high-index classes relative to design-based estimates derived directly from plot classifications. In this way, interpolation may can alter class prevalence relative to design-based estimates.

Considering MOG estimates across all CONUS lands, Herrera *et al* (2025) report 115.54 million ha of mature forest compared to our mean estimate of 154.83 (153.74–155.96), and 2.30 million ha of old-growth compared to our mean estimate of 25.17 (24.47–25.91) million ha. These differences likely reflect how information is propagated and updated across space by each method. Both approaches use FIA plots to characterize MOG occurrence, and in the interpolation framework plot information is propagated spatially without incorporating additional empirical evidence at prediction locations. In our framework, FIA plot information similarly informs spatial prior probabilities of class occurrence. The priors are then updated using remotely sensed information, related to the criteria defining MOG presence, at all prediction locations. How empirical information is incorporated into the prediction frameworks likely contributes to the lower MOG totals estimated by Herrera *et al* (2025), given our estimates are in relative agreement with design-based estimates.

4.3. Model performance

Our forest models were approximately unbiased across the range of predicted probabilities, while the MOG models contained regional positive biases (resulting in over prediction) that increased as the predicted probability increased (figure 7). There are at least two possible causes for the tendency to over-predict large MOG class probabilities. First, we found a pattern in the distribution of aspect values among large predicted MOG probabilities that was not evident in our training data (figure S9). While not all north facing slopes received large predicted old-growth probabilities, hectares with predicted MOG probabilities >80% tended to be on north facing slopes more than expected given the distribution

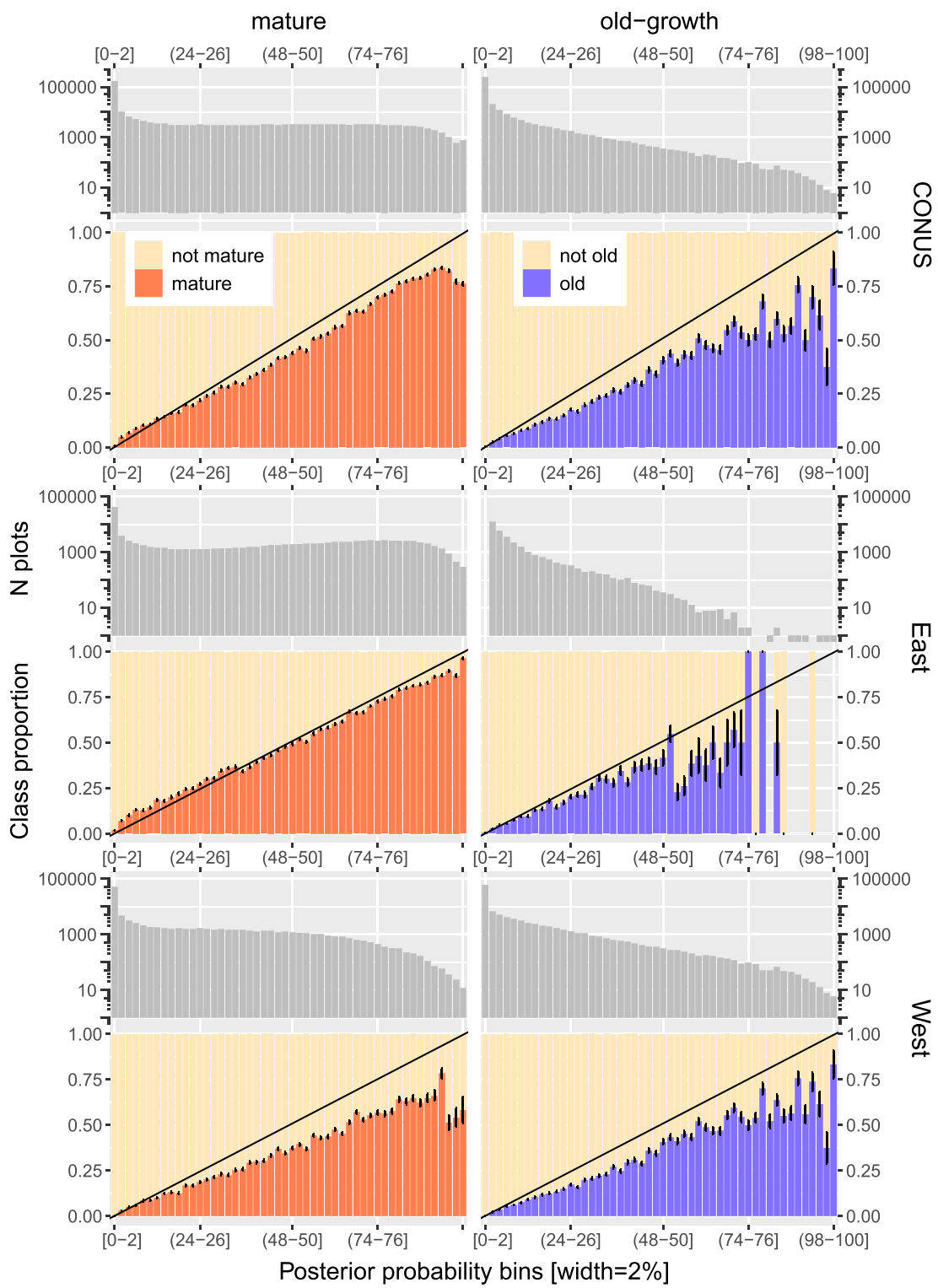

Figure 7. QDA model *k*-fold cross validation results presented for all CONUS, and East (1–13) and West (14–28) strata groupings. All vertical bars represent FIA plots with a predicted probability (binned in 2% intervals on the *x*-axis). The gray bars show the number of plots in each bin on a log scale. The stacked color bar charts show the class proportion (and standard error) of FIA plots within each bin.

of aspects from MOG-labeled plots. Aspect was not considered as a predictor variable due to its inability to conform to a normal distribution upon transformations. Future work could use southness and eastness indices which can be transformed into normal distributions, although it is unclear if that would mitigate this potential issue.

A second potential source of model bias is slight non-normality in the distributions of select predictor variables in some strata (section A.2.2). QDA assumes the predictor variables at a particular location arise from a multivariate normal distribution particular to the classification. Probabilities of class

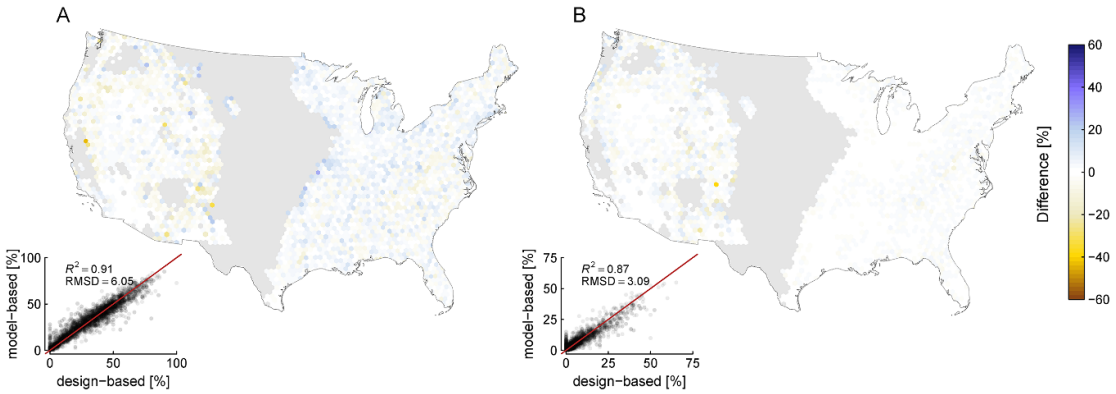

Figure 8. Spatial comparisons of the design-based and model-based MOG estimates across CONUS. The difference between model-based and design-based estimates of mature (A) and old-growth (B) forest amounts (as a percentage of total land area) are mapped across CONUS within approximately 1800 km^2 hexagons. Blue-purple indicates the model-based estimates are larger (model over-prediction), while yellow-brown indicates the model-based estimates are smaller (model under-prediction). Gray-masked hexagons are those with fewer than 5 FIA training plots for the MOG models or had below 10% QDA-estimated forest proportion. The scatter plots show the design-based and model-based estimates from which the differences are calculated.

membership are given by a ratio of the likelihood of the observed predictors originating from each class (equation (A2)). The multivariate normal assumption is analytically and computationally convenient, but if the data are poorly described by a normal distribution, certain ranges of the predictor variables may produce inaccurate ratios and corresponding probabilities that result in under- or overprediction. However, when we compared the normal-derived probabilities to more flexible, non-parametric distribution probabilities, we did not observe compelling differences that would explain the observed biases on the higher end of the probability gradient in figure 7.

Figure 3 indicates empirical model bias was not strong or pervasive enough to yield systematic errors in predicted MOG proportions at the stratum level relative to our training data. While the model-based and design-based estimates depend on the same FIA plot classifications, they arise from different statistical paradigms, precluding a statistical assessment of similarity. Instead, we use estimate comparisons as a heuristic for characterizing spatial patterns of empirical model bias. As is common with model-based inference derived from remote sensing and sparse forest inventories across large areas, we expect localized, sub-stratum biases from within-stratum variation in the predictor-response relationship (e.g. Bruening *et al* 2023, May *et al* 2023). Our biogeographic stratification attempted to mitigate this possibility by striving for homogeneous within-stratum predictor-response relationships, however subtle differences in forest composition or climatic and edaphic characteristics likely persist across relatively short distances. If present, such differences could cause the local predictor-response relationship to deviate from the strata-level relationship and result in local under- and overprediction by the strata-level model. The patterns in figure 8 demonstrate this reality, representing spatially clustered differences between the model-based and design-based MOG proportion estimates, likely arising from localized under- and over-prediction.

4.4. Map interpretation and utility

Class presence in a 1 ha grid cell is inherently binary—either it exists or it does not. Our modeling framework enables inference into this binary possibility based on the degree of similarity between the observed forest characteristics at any given location and the empirically derived forest characteristics of that class according to our training data. In other words, the probability surfaces are a measure of certainty (or uncertainty) about class presence, and the models are more confident in class presence or absence for predicted values closer to 100% or 0% respectively than for values closer to 50%. This also means that class presence is never guaranteed, regardless of the predicted probability value.

Despite the lack of certainty regarding class presence, the probabilities allow inference at a given location relative to other locations. Because one can never be sure of class presence at the 1 ha scale, we also provide coarse predicted proportion estimates at 25 km^2, representing the proportion of hectare pixels in a 5 km by 5 km area that we expect to contain the given class. These estimates are a function of the 1 ha posterior class distributions, and are presented in the form of a mean expected value, with uncertainty bounds expressed as 95% credible intervals. In this way, the credible intervals account for the uncertainty in class presence inherent to the predicted probabilities, allowing additional inference at the landscape-scale.

Alongside the theoretical and statistical rationale for producing area-level proportions to accompany the unit-level probability surfaces, there is a practical motivation as well: providing actionable science data products with clear interpretations to assist in forest stewardship, management, and conservation. A benefit to this coupled dataset is that area-level aggregation of the posteriors produces a data-driven uncertainty envelope that we expect contains the true population parameter 95% of the time. Each 25 km^2 estimate considers 2500 hectares—an area large enough to produce an actionable credible interval, but small enough to support activities and decision making based on the best-available science in most publicly-owned and some privately-owned (e.g. large private land owners, conservation entities, etc) forests. For example, the credible intervals could be used to delineate areas with minimum or maximum allowable amounts of MOG forests necessary for conservation or management, and the accompanying high-resolution probability surface could then be used to identify precise locations for treatment or protection. Such activities may include identifying candidate locations of undiscovered old-growth for ground-truthing, selecting high-probability mature but low-probability old-growth forests to manage for old-growth characteristics, or selecting harvesting locations that maximize mature forest proportion and minimize old-growth forest proportion within lands managed for timber production.

4.5. MOG estimate uncertainty

Transparent uncertainty budgets greatly increase the utility of maps that inform decision making regarding land use in MOG forests. The uncertainty in MOG class proportion represented by our credible intervals comes from two primary sources: spatial variability in the true MOG class occurrence within the estimation unit, and the effectiveness of the QDA classifier based on the training data. The first component depends on the *in situ* land cover and forest structure; it is reasonable to assume a landscape with more homogeneous forest structure would produce a tighter MOG class proportion credible interval, regardless of the actual class membership and predicted proportion, than a more heterogeneous landscape with a large diversity of forest structures. This is also true for other modes of area-level estimation and statistical inference (Patterson *et al* 2019).

The second component depends on within-class variability in the predictors, and the ability of the QDA model to differentiate between classes. The process of extending the inventory-based MOG definitions to a remote sensing context required analytical steps that introduced noise to the relationship between the class labels and response variables, decreasing classifier effectiveness. The credible interval depends on the spread of the posterior distributions, which are impacted by the discriminatory power of the QDA classifier, i.e. the separation in the distribution of predictor variables between the MOG classes training data. An effective discriminator will produce a tighter posterior class distribution centered on the true class (smaller credible interval) than an ineffective discriminator (larger credible interval). Here, we highlight four factors that impact the discriminatory power of our modeling framework, the uncertainty from which is reflected by the credible intervals.

First, MOG classifications are made at the stand level, which we aggregated to the plot level. Second, MOG definition criteria vary by FIA region and forest type, but our modeling framework mixes the classifications within a strata to form a single response variable for each class. Both factors are related to the plot-level classifications (section 2.1), and would reduce model discriminatory power if the relationship between the predictor and response varies between forest stands, forest types, or definition criteria. This is likely true to some extent, as both Bruening *et al* (2023) and May *et al* (2023) demonstrate spatial variations in the relationship between GEDI and FIA data. Third, the temporal mismatch between the inventory sampling and the remote sensing data products could result in structural changes (due to normal forest dynamic processes or external disturbances) between the forest inventory and remotely sensed measurement, which would add noise to the training data. Lastly, measurement and model error associated with the remote sensing predictor variables may have also added variation to the training data. We did not explicitly assess the potential impact of these factors, and instead present them here as sources of uncertainty reflected by the credible intervals.

4.6. Conclusion

The complexity, diversity, scarcity, and longevity of ancient forest landscapes make them among the least understood ecosystems. Younger, maturing forests are perhaps easier to characterize because they tend to exhibit lower structural diversity, are more common, and operate on shorter time scales that allow for a better understanding of developmental trends in structure and functioning. Several related factors make MOG mapping a significant challenge: the diversity of MOG forest characteristics; competing definitions, some of which do not directly translate to remote sensing mapping methods; site-specific forest life history and multi-scale disturbance patterns that are poorly constrained by possible predictor

variables; and the fact that existing MOG forests are not a representative sample of pre-colonial MOG forests and thus our ability to understand the full spectrum of possible MOG structures and functions may be limited. Consistent, long-term management of these forests is similarly constrained by the mismatch between the centuries-long timelines required to develop MOG characteristics and processes and the shorter durations of political administrations and human lifespans. Our findings, therefore, are not a definitive answer to the science questions that inspired this work, but rather a probabilistic, model-based interpretation of empirical data related to this enduring challenge at a specific snapshot in time.

The spatial resolutions at which we provide inference make the work significant from both basic and applied science perspectives. Our 25 km^2 estimates are more than 1.5 orders of magnitude finer than the national inventory estimates, yet retain a clear uncertainty budget. The 1 ha probability surfaces complement the 25 km^2 estimates by providing spatially precise information necessary for management and conservation at an appropriate resolution—a critical but often overlooked element of forest attribute mapping (Duncanson *et al* 2025). Our characterization of MOG spatial patterns—unattainable from inventory data alone—was designed to support real-world management and conservation decisions with transparent statistical inference. However, while structural MOG definitions lend themselves well to mapping via remote sensing, they exclude old forests that do not conform to the structural criteria Bruening *et al* (2024), see supporting information and. Accordingly, classification-style definitions like those used here may not fully capture forests containing the oldest trees (Spies 2004, Pesklevits *et al* 2011, Moore and Nelson 2023).

Ensuring the future of MOG forests requires more than improved definitions, data, or models—it demands humility and a fundamental shift in how we understand and interact with these ecosystems. Integrating Indigenous and Western forest knowledge through bilateral partnerships (Lertzman 2010, Eisenberg *et al* 2024), embracing ecological complexity and diversity, and building long-term, adaptive frameworks from place-based quantative and qualitative information are not aspirational goals but urgent necessities. Without such a transformation, our conservation and management strategies risk falling short of what these ecosystems require to persist.

Acknowledgments

We thank the entire Forest Structure Data Partnership at the U.S. Forest Service for their enthusiasm and support of our work; Drs. Christina Eisenberg and Susan Prichard for discussions related to Indigenous Knowledge and data sovereignty; and Kevin Barnett and Drs. Greg Aplet and Peter Nelson for years of MOG-related discussions that have indirectly shaped our work. Additionally, we thank the University of Maryland's DIT-CUIE team for their technical support with the CUI computing environment.

Data availability statement

The data that support the findings of this study are openly available at the following URL/DOI: https://doi.org/10.3334/ORNLDAAC/2498 (Bruening *et al* 2026).

Supplementary Data 1 available at https://doi.org/10.1088/2752-664X/ae5300/data1.

Funding

This work was supported by funding from the Global Ecosystem Dynamics Investigation (NASA contract NNL15AA03C) and from the United States Forest Service (Grant No. 23CS11132420412).

Conflict of interest statement

The authors have no conflicts of interest to report.

Ethics statement

This research did not involve human or animal participants.

Author contributions

Jamis M Bruening 0000-0002-9750-7806
Conceptualization (equal), Data curation (lead), Formal analysis (lead), Investigation (lead), Methodology (equal), Software (equal), Validation (equal), Visualization (lead), Writing – original draft (lead), Writing – review & editing (lead)

Paul B May
Conceptualization (supporting), Formal analysis (supporting), Investigation (supporting), Methodology (equal), Software (equal), Validation (equal), Writing – review & editing (supporting)

Ralph O Dubayah 0000-0003-1440-6346
Conceptualization (equal), Funding acquisition (lead), Investigation (supporting), Supervision (lead), Writing – review & editing (supporting)

Luke Wertis
Data curation (supporting), Formal analysis (supporting), Software (supporting)

Colin Quinn 0000-0001-7813-690X
Data curation (supporting), Software (supporting), Writing – review & editing (supporting)

Neil Pederson
Conceptualization (supporting), Funding acquisition (equal), Investigation (supporting), Supervision (supporting), Writing – original draft (supporting), Writing – review & editing (supporting)

Amanda H Armstrong 0000-0002-9123-8924
Investigation (supporting), Writing – review & editing (supporting)

Ben Poulter
Funding acquisition (equal), Supervision (supporting), Writing – review & editing (supporting)

Appendix. Methods

The following sections compliment section 2.2 of the main manuscript, providing more detail regarding our implementation of spatial QDA, the necessary modifications to adapt classical QDA to MOG mapping in a spatially explicit framework, pre- and post-processing, our biogeographic stratification, and the remote sensing predictor variables

A.1. Remote sensing predictor variables

The national MOG definitions rely on a set of physical and structural stand attributes that are impacted by successional development over decades to millennia. Here, we are not evaluating the efficacy of structural attributes as MOG definition criteria (although implications are presented in the discussion and supplementary material); instead, we have designed a quantitative mapping framework that is tailored to the phenomena we are trying to map (see figure 9 in Bruening *et al* 2024). In this case, MOG status is defined primarily by structural attributes (table 1), and we extend this logic to our mapping framework by considering a suite of predictor variables that represent various forest structural attributes related to the MOG definitions, and to a lesser extent, functional and temporal attributes. The variables are organized into two distinct data types: point-location waveform lidar measurements of vertical forest structure from the GEDI mission (Dubayah *et al* 2020), and wall-to-wall gridded data sets representing other forest and topographic attributes.

A.1.1. GEDI data

Our base modeling unit was an FIA plot, and thus our predictor variables needed to represent the forest characteristics at the exact plot locations. A common challenge in linking data from remote sensing sampling missions, such as GEDI, with forest inventory data is the low-probability of an exact spatial collocation between an inventory plot and the remotely sensed measurement. This is especially true given geolocation uncertainty, and a mismatch in geometries between a GEDI footprint (a circle of approximately 490 m^2), and the four circular, clustered subplots that make up a single FIA plot (combined, approximately 675 m^2) (see figure 1 in May *et al* 2024). To mitigate these challenges, May *et al* (2024) developed a method of GEDI waveform imputation for the FIA plot network. This method enables prediction of GEDI waveforms and associated uncertainties at the FIA plot centers, while preserving the hidden nature of the FIA plot coordinates. The GEDI predictions can be used to model FIA

plot-level forest attributes, and the authors provide an example application for mapping aboveground biomass density. Their results indicate the waveform prediction method generally performs well, matching true GEDI observations and credible uncertainty estimates. They show regional variation in prediction accuracy and uncertainty, primarily dependent on GEDI sample density; regions in the eastern US tended to have higher prediction variance due to lower sample density. Across three validation regions, the 95% credible intervals achieved near-nominal coverage (95%) for most waveform height metrics, indicating that the model's predicted uncertainties are well-calibrated and that waveform shapes are realistically reproduced via cross-validation. Some waveform height metrics showed slight overconfidence and higher relative variance in regions with lower GEDI sample density.

We used the data and R code for GEDI prediction from May *et al* (2025) to produce two GEDI variables at the FIA plot locations to be considered among the other candidate MOG predictor variables in model training; 1) a common proxy for maximum canopy height (referred to as rh98) and 2) a lidar metric called the vertical distribution ratio (VDR), quantified as the normalized ratio [0–1] between the maximum and median relative heights (VDR = (rh98 - rh50)/rh98) of the predicted waveform (Goetz *et al* 2007). Stands with a dense upper canopy and sparse lower canopy have relatively low VDR, whereas stands with a more even vertical distribution of vegetation have relatively larger VDR's.

GEDI level 2A data were used to make predictions when applying the models to predict the posterior MOG class distributions within the 1 ha spatial grid (Dubayah *et al* 2021). These data were collected between April 2019 and March 2023, and filtered for quality using the level 2A quality filter and additional filtering from Bruening *et al* (2023). For each strata's model calibration, we selected a single GEDI variable for inclusions as a predictor due to a high degree of correlation between GEDI metrics.

A.1.2. Gridded data

Six sources of wall-to-wall gridded remote sensing data and derived products were considered as candidate MOG predictor variables: 30 m Landsat composite images from 2022 (Hansen *et al* 2013); 30 m phenology time series derived from seasonal enhanced vegetation index (EVI) curves from Landsat Sentinel-2 fusion (Friedl 2020); 25 m ALOS PALSAR-2 L-band SAR HH and HV polarization mosaics (JAXA 2018); 10 m canopy surface texture metrics derived from a 2022 Sentinel-2 EVI composite processed on Google Earth Engine; a 10 m canopy height model derived from GEDI-Sentinel-2 fusion (Lang *et al* 2023); and 25 m topographic variables generated from the SRTM digital elevation model (JPL 2013). Across these six data sources, a total of twenty candidate predictor variables were generated (table S2). All candidate predictor variables were spatially aggregated from their native resolutions (10–30 m) to the 1 ha modeling grid using GDAL's area-weighted average resampling, producing values representing the mean conditions within each 1 ha pixel. This approach ensures consistency between predictor support and model resolution and avoids bias associated with interpolative resampling methods. Because the target grid resolution is not an exact multiple of the native predictor grid resolutions, area-weighted aggregation also appropriately accounts for partial pixel overlaps, providing a principled representation of sub-pixel heterogeneity.

A.2. Spatial QDA

A.2.1. Biogeographic stratification

A major factor in the success of modeling forest attributes from remote sensing data is a consistent relationship between predictor and response variables throughout the study area (May *et al* 2023). Evidence suggests that relationships between GEDI forest structure measurements and aboveground biomass density vary substantially across space within CONUS (Bruening *et al* 2023). Similarly, it is reasonable to assume spatial variation in the relationship between remote sensing data and MOG forest conditions, given MOG status is dependent on a host of spatially-varying factors such as forest type, species composition, climate, and disturbance history (Spies and Franklin 1996). To reduce the impact of this variation in our modeling framework, we stratified CONUS into 29 different biogeographic strata (figure 9). Our intent was to minimize spatial variation in the relationships between MOG predictor and response variables within a strata, while also retaining enough FIA plots in each class to enable model calibration (table S3 and figure 2). We considered the following factors in delineating the strata: 1) Levels 2 and 3 U.S. Environmental Protection Agency ecoregional boundaries (Omernik and Griffith 2014), 2) maintaining at least 100 plots in each of the four modeled classes (non-forest, old-growth forest, mature forest, and other forest), 3) *a priori* knowledge of large-scale spatial trends in forest composition, biogeography, land-use history, and climate.

We also considered stratifying CONUS by forest composition (e.g. FIA forest type 'FORTYPCD'), but ultimately decided against it for two reasons: first, not all forest types contained enough response forest

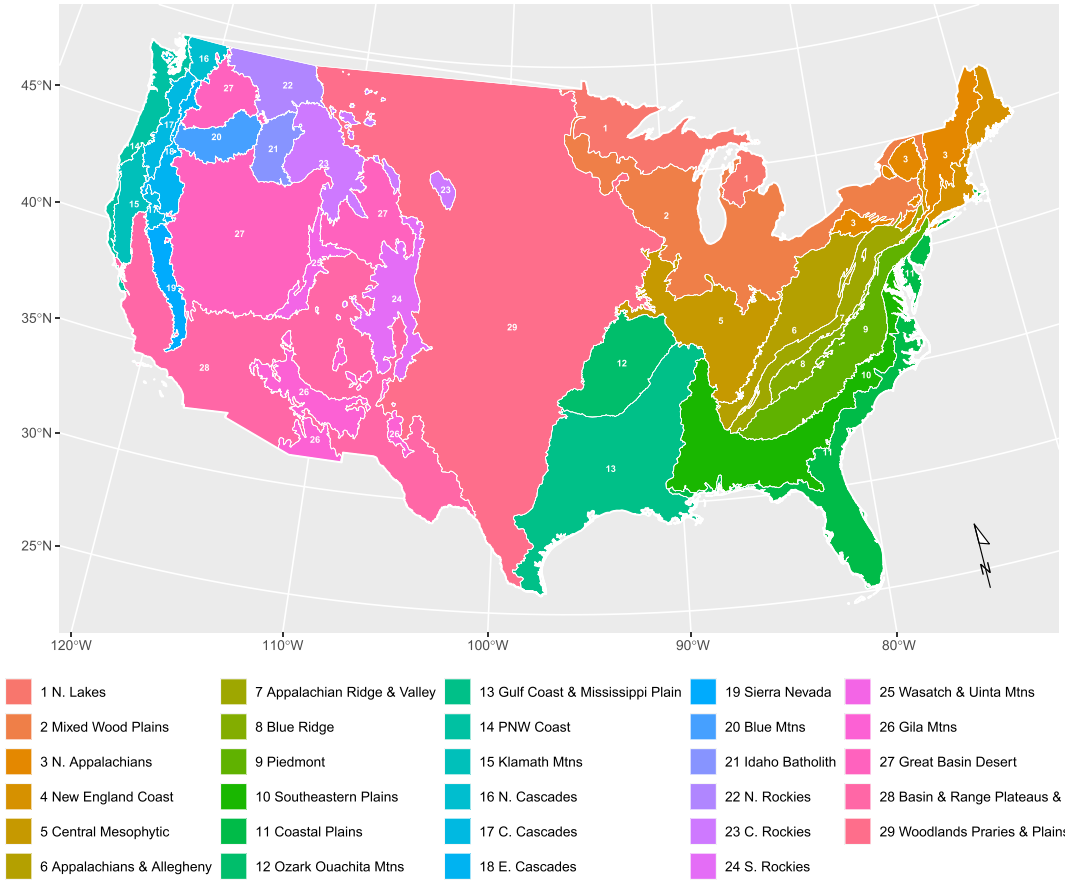

Figure 9. Ecoregional stratification of CONUS used to calibrate and apply localized MOG models. The models were calibrated using all FIA plots within the strata boundaries, and then applied to all ha pixels within the strata boundaries.

variable labels ('old-growth', 'mature', or 'other') to enable robust model calibration; second, spatially continuous and well-validated maps of these forest classes are not available at the spatial resolution of our mapping framework, and resampling would introduce methodological complexity and noise to our training data. We avoided these limitations by opting for a more straightforward biogeographic stratification approach.

A.2.2. Pre-processing

The national MOG definitions are contingent on the presence of forest—an FIA stand must be forested to be eligible for mature or old-growth classification. Similarly, the mature definitions were developed so that any FIA stand classified as old-growth necessarily meets the mature criteria as well. Thus, the classes are nested in that all stands classified as old-growth forest also meet the definition of mature forest, and all MOG stands meet the definition of forest. Given 1) the lack of *a priori* knowledge about the occurrence of these classes outside the FIA plot boundaries, 2) their nested hierarchy, and 3) the ecological theory of forest stand development that underpins the MOG definitions, we designed a nested classification modeling framework to predict the probability of each of the following nested categories individually: 1) all forest, 2) mature or old-growth forest, and 3) only old-growth forest. Using the FIA plot-level classifications we created three separate binary response variables, one for each of the aforementioned nested modeling categories, each of which served as a response variable in QDA model training. The private FIA plot coordinates were used to extract values from the 1 ha gridded remote sensing predictors in a secure Controled Unclassified Information computing environment, and were combined with the predicted GEDI variables (from section A.1.1) and the three binary response variables to form the QDA training data set used for model calibration within each strata.

Quadratic discrimination analysis requires the predictor data to be distributed multivariate normal within each class. We evaluated normality through visual assessment of the candidate predictor variables in each of the four classes. Transformations were applied when needed, and variables were removed for a given stratum's model if normality was not obviously achieved, or if there was no discriminatory power

relative to class membership across the three binary response variables. We allowed minor to moderate non-normality in the distributions for variables that presented substantial discriminatory power across the response variable classes; we deemed limited violations of the normality assumption to be worth substantial gains in discriminatory power. The final list of variables used for each stratum are reported in table S2. Each selected predictor was centered (subtracted from the sample mean) and scaled (divided by the sample standard deviation) to make the predictors unit-less and have similar scales of variation, which is critical for the principal component projections discussed next.

The last pre-processing step was dimensionality reduction in the final set of gridded predictor variables via principal component analysis (PCA). Using principal component projections of the final remote sensing variable as model predictors improved the cross-validated QDA model performance relative to models fit using the original variables, and reduced model complexity by decreasing the number of independent variables used. Across the 29 strata, the number of gridded remote sensing variables prior to PCA projections ranged between 7–17, and models fit using the first two principal components achieved similar performance. Importantly however, the predicted GEDI waveform metrics were excluded from the PCA projections. GEDI observations were not available in every 1 ha grid cell, as GEDI samples forest structure at locations along the ISS orbital track instead of recording wall-to-wall measurements (Dubayah *et al* 2022). Thus, we excluded the GEDI waveform variable from PCA dimensionality reduction during QDA model training to ensure the principal component projections could be used when applying the QDA models in pixels without on-orbit GEDI data. Accordingly, the three variables used in each strata's QDA calibration were the first two principle components of the gridded remote sensing variables and the single selected GEDI waveform variable (section A.1.1). Our approach enabled posterior class distributions to be generated for all 1 ha grid cells, regardless of the presence of a GEDI measurement, as QDA can handle missing predictor variables. When applying the QDA models, GEDI data and the first two principal components were used in 1 ha pixels that contained a GEDI observation, and in all other cells only the principal components were used. A drawback of using principle components was that the projections clouded our ability to differentiate between individual predictor variables' model importance in the QDA models, which we deemed a worthwhile tradeoff for increased model performance achieved using PCA predictors.

A.2.3. Spatial QDA model development and training

QDA assumes the predictor variables follow a multivariate normal distribution specific to the underlying classification:

$$\boldsymbol{X}|\,(C=k) \sim \mathrm{MVN}\,(\boldsymbol{\mu}_k, \boldsymbol{\Sigma}_k); \quad k=0,\ldots,K-1 \tag{A1}$$

where $\boldsymbol{X}$ is a vector of predictor variables and $C=0,\ldots,K-1$ represent the K potential classes. Given a fixed class, $C=k$, the predictor values are assumed to be multivariate normal with class-specific mean and covariance matrix $\boldsymbol{\mu}_k$ and $\boldsymbol{\Sigma}_k$ respectively. As is typical, our class labels are sparsely observed across space while the predictor variables are continuously available. The goal is to compute the posterior probability of a given class label given the observed predictors,

$$\mathrm{Prob}\,(C=k|\boldsymbol{X}) = \frac{f(\boldsymbol{X}|C=k)\,\pi_k}{\sum_{j=0}^{K-1} f(\boldsymbol{X}|C=j)\,\pi_j}, \tag{A2}$$

where $f(\boldsymbol{X}|C=k)$ is the probability of the observed predictors originating from class k and π_k is the prior probability of class k's occurrence. The posterior probability is a product of these two factors, normalized by the sum of this same product for all possible classes. Broadly speaking, the lower the prior probability of class k, the more compelling the predictors must be to result in a substantial posterior probability—the predictors must be compelling in the sense that the likelihood of originating from class k greatly exceeds the likelihood of originating from the other $K-1$ classes. Note the probability in (A2) is also conditional on some unknown parameters, thus far $\boldsymbol{\mu}_k,\ \boldsymbol{\Sigma}_k,\ \pi_k$ for $k=0,\ldots,K-1$. We temporarily omit this conditioning from our notation for simplicity.

Two important adaptations must be made from classical QDA to fit our task. First, classical QDA assumes the classes are disjoint, whereas in this setting they are partially nested (i.e. all mature forest is forest and all old-growth forest is mature forest). To address this hierarchy, we posed a set of nested binary classifications. First, a binary QDA is used to discriminate between forest and non-forest. Given a location is forest-class, a second binary QDA is used to discriminate between MOG forest (MOG classes) and other forest. Given MOG-class, a third binary QDA is used to discriminate between old-growth forest and mature forest classes. Explicitly, we pose

$$\boldsymbol{X}|\left(C_0=k\right)\sim \mathrm{MVN}\left(\boldsymbol{\mu}_{0,k},\boldsymbol{\Sigma}_{0,k}\right);\quad k=0,1 \qquad \text{(non-forest/forest)} \tag{A3}$$

$$\boldsymbol{X}|\left(C_0=1,\ C_1=k\right)\sim \mathrm{MVN}\left(\boldsymbol{\mu}_{1,k},\boldsymbol{\Sigma}_{1,k}\right);\quad k=0,1 \qquad \text{(other/MOG)} \tag{A4}$$

$$\boldsymbol{X}|\left(C_0=1,\ C_1=1,\ C_2=k\right)\sim \mathrm{MVN}\left(\boldsymbol{\mu}_{2,k},\boldsymbol{\Sigma}_{2,k}\right);\quad k=0,1 \qquad \text{(mature/old-growth)}, \tag{A5}$$

respectively for the forest, MOG (mature or old-growth), and old-growth only forest classes, where $k=0$ denotes negative class status and $k=1$ denotes affirmative class status, granting access to the next stage of consideration. Likewise, prior probabilities $\pi_{0,k},\ \pi_{1,k},\ \pi_{2,k}$ for $k=0,1$ are nested, e.g. $\pi_{2,1}$ is the prior probability of old-growth given MOG. An affirmative class status from previous discriminatory stages is never known with certainty—to compute posterior probabilities for latter stages, we back-propagated through the previous affirmative probabilities: Posterior probabilities for non-forest/forest, $\mathrm{Prob}(C_0=k|\boldsymbol{X})$, can be computed as in (A2). We then have

$$\mathrm{Prob}\left(C_1=k|\boldsymbol{X}\right)=\mathrm{Prob}\left(C_1=k|C_0=1,\boldsymbol{X}\right)\cdot\mathrm{Prob}\left(C_0=1|\boldsymbol{X}\right) \tag{A6}$$

$$\mathrm{Prob}\left(C_2=k|\boldsymbol{X}\right)=\mathrm{Prob}\left(C_2=k|C_1=1,\boldsymbol{X}\right)\cdot\mathrm{Prob}\left(C_1=1|\boldsymbol{X}\right). \tag{A7}$$

Our second QDA adaption addresses spatial autocorrelation inherent to forest class mapping. Classical QDA assumes both fixed prior probabilities and, given a fixed class label, independent realizations of $\boldsymbol{X}$. Yet, neither of these assumptions are appropriate in a spatial context. Our forest classes of interest are spatially clustered (e.g. old-growth forest is more likely located near other old-growth forest than near non-forest). Similarly, given a fixed class label, we expect realizations of $\boldsymbol{X}$ from nearby locations to be more similar than those from more distant locations. As such, we adapted the prior probabilities to reflect local clustering and large scale spatial variation, as the scale and magnitude of spatial variation can be inferred from the observed class labels at the FIA plot locations. The spatial variation in $\boldsymbol{X}$ can also be inferred from the known class labels and associated values of $\boldsymbol{X}$ at the FIA plot locations. Here we use Gaussian processes as the mathematical structure to account for both of these factors, as follows (Gelfand and Schliep 2016).

Let $\boldsymbol{s}$ represent a location within our analysis area (a stratum). Starting with the prior probabilities, we assume of the affirmative probabilities

$$\pi_{j,1}\left(\boldsymbol{s}\right)=\mathrm{softmax}\left(\mu_{\pi,j}+w_{\pi,j}\left(\boldsymbol{s}\right)\right);\quad j=0,1,2 \tag{A8}$$

where $\mu_{\pi,j}$ is a constant intercept and $w_{\pi,j}(\boldsymbol{s})$ is a mean-zero Gaussian process with Matérn covariance (Genton 2001, equation (12) governed by unknown correlation parameters $\boldsymbol{\phi}_{\pi,j}$. The softmax function is used to map the unconstrained argument to valid probabilities between 0 and 1. The negatory probabilities are then $\pi_{j,0}(\boldsymbol{s})=1-\pi_{j,1}(\boldsymbol{s})$.

A similar approach is taken to the class-fixed predictor values:

$$\boldsymbol{X}\left(\boldsymbol{s}\right)|\left(C_0\left(\boldsymbol{s}\right)=k\right)=\boldsymbol{\mu}_{0,k}+\boldsymbol{w}_{0,k}\left(\boldsymbol{s}\right);\quad k=0,1 \tag{A9}$$

$$\boldsymbol{X}\left(\boldsymbol{s}\right)|\left(C_0\left(\boldsymbol{s}\right)=1,\ C_1\left(\boldsymbol{s}\right)=k\right)=\boldsymbol{\mu}_{1,k}+\boldsymbol{w}_{1,k}\left(\boldsymbol{s}\right);\quad k=0,1 \tag{A10}$$

$$\boldsymbol{X}\left(\boldsymbol{s}\right)|\left(C_0\left(\boldsymbol{s}\right)=1,\ C_1\left(\boldsymbol{s}\right)=1,\ C_2\left(\boldsymbol{s}\right)=k\right)=\boldsymbol{\mu}_{2,k}+\boldsymbol{w}_{2,k}\left(\boldsymbol{s}\right);\quad k=0,1 \tag{A11}$$

where $\boldsymbol{w}_{j,k}$ for $j=0,1,2;\ k=0,1$ are multivariate Gaussian processes with variance $\boldsymbol{\Sigma}_{j,k}$ and correlation parameters $\phi_{j,k}$. For any fixed location, equations (A9)–(A11) are equivalent to equations (A3)–(A5), but the Gaussian processes allow for spatial correlation between nearby $\boldsymbol{X}$ that share class labels.

For a desired prediction location $\boldsymbol{s}_*$, the posterior probability in equation (A2) is dependent on a number of unknown model parameters and effects. Letting $\boldsymbol{\theta}$ be the concatenation of these unknowns, the left side of equation (A2) is better represented as $\mathrm{Prob}(C=k|\boldsymbol{X},\boldsymbol{\theta})$. We take a Bayesian approach to statistical inference (Gelman and Rubin 1995), where equation (A2) is integrated across the distribution of possible parameters/effects, conditional on our observed data. Let $\mathcal{D}$ be the observed data set. Then

$$\mathrm{Prob}\left(C_j\left(\boldsymbol{s}_*\right)=k|\boldsymbol{X}\left(\boldsymbol{s}_*\right),\mathcal{D}\right)=\int_{\boldsymbol{\theta}\in\Theta}\mathrm{Prob}\left(C_j\left(\boldsymbol{s}_*\right)=k|\boldsymbol{X}\left(\boldsymbol{s}_*\right),\ \boldsymbol{\theta}\right)\cdot p\left(\boldsymbol{\theta}|\mathcal{D}\right)\ \mathrm{d}\boldsymbol{\theta}, \tag{A12}$$

where $p(\boldsymbol{\theta}|\mathcal{D})$ is the posterior distribution of the model unknowns given the observed data. Computing this posterior distribution is the Bayesian version of 'model training':

$$p\left(\boldsymbol{\theta}|\mathcal{D}\right)\propto f(\mathcal{D}|\boldsymbol{\theta})\,\pi\left(\boldsymbol{\theta}\right), \tag{A13}$$

where $f(\mathcal{D}|\boldsymbol{\theta})$ is the data probability determined by the assumed model and $\pi(\boldsymbol{\theta})$ represents the prior beliefs on the model unknowns. We assumed uninformative priors for all parameters, allowing the data

to dictate our posterior beliefs. As is typical in Bayesian inference, the integral in (A12) cannot be evaluated analytically. We used Monte Carlo methods to draw a set of random samples from equation (A13), which we refer to throughout this paper as the posterior distribution of class occurrence for a given hectare. Finally, we calculated the probability of a given class's occurrence by evaluating equation (A12) numerically.

A.2.4. Area-level estimation and uncertainty quantification

We produced area-level aggregations to generate total and mean estimates with uncertainty, quantified using a 95% credible interval, at national, stratum, and 25 km^2 spatial scales. The estimates represent the total or proportion of hectares within spatial estimation unit that contain the given class. Again, we used Monte Carlo methods to approximate these quantities. For a given spatial estimation unit $\mathcal{A}$, random samples from the joint posterior of $\{C_j(\boldsymbol{s});\ \boldsymbol{s} \in \mathcal{A}\}$ were generated. Each sample represents a posterior-plausible configuration of presence/absence of class j across area $\mathcal{A}$. These samples were composed into samples of the area total as $C_j(\mathcal{A}) = \sum_{\boldsymbol{s}\in\mathcal{A}} C_j(\boldsymbol{s})$. Samples of the area mean were produced by dividing $C_j(\mathcal{A})$ samples by the number of hectare pixels in $\mathcal{A}$. Expected values and 95% credible intervals were approximated by taking the sample average and sample $(2.5, 97.5)\%$ quantiles of Monte Carlo samples, respectively.

We generated direct, design-based class proportion estimates from our FIA training data for comparison with our model-based proportion estimates (figures 3 and 8). We followed the approach outlined in (section 2.1 in May *et al* 2023) for mean and variance estimation, adapted for proportions

$$\hat{p}_X = \frac{1}{n}\sum_{i=1}^{n} X_i \tag{A14}$$

and

$$\widehat{V}(\hat{p}_X) = \frac{1}{n(n-1)}\sum_{i=1}^{n}(X_i - \hat{p}_X)^2 \tag{A15}$$

where n is the number of FIA plots per strata and $X_i \in \{0,1\}$ is the binary class indicator for plot i.

A.2.5. Cross-validation

We performed 10-fold cross validation of our modeling routine for each stratum using randomly partitioned folds. For each partition we calibrated the QDA model using the nine remaining folds, and made predictions at the locations of the withheld fold's FIA plots. This process was repeated across all partitions within a strata, and performed for all 29 strata individually. Aggregated results are reported in figure 7 at the national and regional scales, and stratum-level results in figures S4–S8. This was our primary method of assessing model performance at the stratum-level during model calibration; in designing our modeling framework and selecting final models, the stratum-level cross validation results served as our primary justification in decision making.

In this instance, our QDA models were not used to spatially extrapolate outside the area that encompassed the training data. Rather, we used the models to interpolate between the FIA plots: in eastern strata our training data was evenly distributed entirely throughout each modeling strata; and in western strata, almost all forested land fell within federal land boundaries where the MOG classifications were available (figure S2). While there is evidence of over-confidence in biophysical forest modeling exercises that do not account for spatial autocorrelation in model validation, such as spatially clustered data partitions (e.g. Ploton *et al* 2020), this applies when models are used to predict into 'unknown space' where the new predictor data could be different from the training data (Meyer and Pebesma 2021). This is not the case with our analysis, as our training data locations are a spatially uniform random sample of the CONUS landscape (Bechtold and Patterson 2005).

A.2.6. Post-processing

To reduce the potential for confusion and to simplify interpretation and increase the utility of our maps, we separated results for the the MOG classes into mutually exclusive classes (instead of the nested classes necessary for modeling, see section A.2.2). Thus, while the forest class results refer to all forest classes (old-growth, mature, and other), the MOG results presented throughout the paper refer to disjoint classes. After generating the posterior distributions within the 1 ha spatial grid, we calculated a mature-only forest class probability map and area-level estimates, defined as

$$\text{Prob}\left(C_{\text{mature}}\right) = \text{Prob}\left(C_{\text{MOG}} = k|\boldsymbol{X}\right) - \text{Prob}\left(C_{\text{old-growth}} = k|\boldsymbol{X}\right). \tag{A16}$$

References

Adlam C, Almendariz D, Goode R W, Martinez D J and Middleton B R 2022 Keepers of the flame: supporting the revitalization of indigenous cultural burning *Soc. Nat. Res.* **35** 575–90

Ager A A, Day M A, Ringo C, Evers C R, Alcasena F J, Houtman R M, Scanlon M and Ellersick T 2021 Development and application of the fireshed registry *Gen. Tech. Rep.* RMRS-GTR-425 (US Department of Agriculture, Forest Service, Rocky Mountain Research Station) **47** 425

Armstrong C G, Earnshaw J and McAlvay A C 2022 Coupled archaeological and ecological analyses reveal ancient cultivation and land use in Nuchatlaht (nuu-chah-nulth) territories, Pacific Northwest *J. Archaeol. Sci.* **143** 105611

Barndt S et al 2023 Mature and old-growth forests: definition, identification, and initial inventory on lands managed by the forest service and bureau of land management

Barnett K, Aplet G H and Belote R T 2023 Classifying, inventorying and mapping mature and old-growth forests in the United States *Front. Forests Global Change* **5** 1070372

Bauhus J, Puettmann K and Messier C 2009 Silviculture for old-growth attributes *Forest Ecol. Manage.* **258** 525–37

Bechtold W A and Patterson P L 2005 *The Enhanced Forest Inventory and Analysis Program–National Sampling Design and Estimation Procedures* (USDA Forest Service, Southern Research Station)

Bruening J M, Dubayah R O, Pederson N, Poulter B and Calle L 2024 Definition criteria determine the success of old-growth mapping *Ecol. Indicators* **159** 111709

Bruening J M, May P B, Armston J D and Dubayah R O 2023 Precise and unbiased biomass estimation from gedi data and the us forest inventory *Front. Forests Global Change* **6** 1149153

Bruening J M, May P B, Dubayah R O, Wertis L, Quinn C, Pederson N, Armstrong A and Poulter B 2026 Mature and old-growth forest probability maps for the conterminous United States *ORNL DAAC* (https://doi.org/10.3334/ORNLDAAC/2498)

Davis M 1996 *Eastern old-Growth Forests: Prospects for Rediscovery and Recovery* (Island Press)

DellaSala D A, Mackey B, Norman P, Campbell C, Comer P J, Kormos C F, Keith H and Rogers B 2022 Mature and old-growth forests contribute to large-scale conservation targets in the conterminous United States *Front. Forests Global Change* **5** 979528

Dubayah R *et al* 2020 The global ecosystem dynamics investigation: high-resolution laser ranging of the earth's forests and topography *Sci. Remote Sens.* **1** 100002

Dubayah R *et al* 2022 GEDI launches a new era of biomass inference from space *Environ. Res. Lett.* **17** 095001

Dubayah R, Hofton M, Blair J, Armston J, Tang H and Luthcke S 2021 GEDI L2A elevation and height metrics data global footprint level v002 *NASA EOSDIS Land Processes DAAC* (https://doi.org/10.5067/GEDI/GEDI02_A.002)

Duncanson L *et al* 2022 Aboveground biomass density models for NASA's Global Ecosystem Dynamics Investigation (GEDI) lidar mission *Remote Sens. Environ.* **270** 112845

Duncanson L *et al* 2025 Spatial resolution for forest carbon maps *Science* **387** 370–1

Eisenberg C Prichard S, Nelson M P and Hessburg P 2024 Braiding indigenous and western knowledge for climate-adapted forests: an ecocultural state of science report

Eisenberg C *et al* 2019 Out of the ashes: ecological resilience to extreme wildfire, prescribed burns and indigenous burning in ecosystems *Front. Ecol. Evol.* **7** 436

Executive Order 14072 2022 Exec. order no. 14072, Strengthening the nation's forests, communities, and local economies

Executive Order 14223 2025 Exec. order no. 14223, Addressing the threat to national security from imports of timber, lumber, and their derivative products

Executive Order 14225 2025 Exec. order no. 14225, Immediate expansion of american timber production

Foster D R and Aber J D 2004 *Forests in Time: the Environmental Consequences of 1,000 Years of Change in New England* (Yale University Press)

Friedl M A 2020 Musli multi-source land surface phenology yearly North America 30 m v011 *NASA EOSDIS Land Processes DAAC*

Frye E A, Copenheaver C A, Gallagher A M and Wiseman P E 2025 Scientific definitions and measurements of second-growth, mature and old-growth forests *J. Forestry* **123** 23–39

Gaines G, Arndt P, Croy S, Devall M, Greenberg C, Hooks S, Martin B, Neal S, Pierson G and Wilson D 1997 Guidance for conserving and restoring old-growth forest communities on national forests in the southern region. *Forestry Report R8-FR* vol 62

Gelfand A E and Schliep E M 2016 Spatial statistics and gaussian processes: a beautiful marriage *Spat. Stat.* **18** 86–104

Gelman A and Rubin D B 1995 Avoiding model selection in Bayesian social research *Sociol. Methodol.* **25** 165–73

Genton M G 2001 Classes of kernels for machine learning: a statistics perspective *J. Mach. Learn. Res.* **2** 299–312

Goetz S, Steinberg D, Dubayah R and Blair B 2007 Laser remote sensing of canopy habitat heterogeneity as a predictor of bird species richness in an eastern temperate forest, USA *Remote Sens. Environ.* **108** 254–63

Gray A N, Pelz K, Hayward G D, Schuler T, Salverson W, Palmer M, Schumacher C and Woodall C W 2023 Perspectives: the wicked problem of defining and inventorying mature and old-growth forests *Forest Ecol. Manage.* **546** 121350

Guala G F, Hua H, Duncanson L I, Niemoeller S C, Hunka N, Mandel A I and Freitag B M 2024 Biomass harmonization and sar analysis with the multi-mission algorithm and analysis platform (MAAP) *WGISS (Working Group on Information Systems and Services) 57th Meeting*

Hansen M C *et al* 2013 High-resolution global maps of 21st-century forest cover change *Science* **342** 850–3

Herrera D J, Schalk C M, Gray A N, Woodbridge M, Olson D H and Cove M V 2025 Leveraging United States forest inventory analysis data to project mature and old-growth forest conditions, with three wildlife case studies showing utility *Forest Ecol. Manag.* **596** 123085

Hilbert J and Wiensczyk A 2007 Old-growth definitions and management: a literature review *J. Ecosyst. Manage.* **8** 16–25

Hoffman K M, Davis E L, Wickham S B, Schang K, Johnson A, Larking T, Lauriault P N, Quynh Le N, Swerdfager E and Trant A J 2021 Conservation of Earth's biodiversity is embedded in indigenous fire stewardship *Proc. Natl Acad. Sci.* **118** e2105073118

Hunka N *et al* 2023 On the NASA GEDI and ESA CCI biomass maps: aligning for uptake in the unfccc global stocktake *Environ. Res. Lett.* **18** 124042

JAXA 2018 Global PALSAR-2/PALSAR/JERS-1 Mosaic and forest/non-forest map (available at: www.eorc.jaxa.jp/ALOS/en/palsar_fnf/data/index.htm)

Keeton W S 2006 Managing for late-successional/old-growth characteristics in northern hardwood-conifer forests *Forest Ecol. Manage.* **235** 129–42

Lake F K and Christianson A C 2020 Indigenous fire stewardship *Encyclopedia of Wildfires and Wildland-Urban Interface (WUI) Fires* (Springer) pp 714–22

Lang N, Jetz W, Schindler K and Wegner J D 2023 A high-resolution canopy height model of the Earth *Nat. Ecol. Evol.* **7** 1778–89
Lertzman D A 2010 Best of two worlds: traditional ecological knowledge and western science in ecosystem-based management *J. Ecosyst. Manage.* **10** 104–26
Long J W, Lake F K and Goode R W 2021 The importance of indigenous cultural burning in forested regions of the pacific west, USA *Forest Ecol. Manage.* **500** 119597
May P B, Dubayah R O, Bruening J M and Gaines G C 2024 Connecting spaceborne lidar with NFI networks: a method for improved estimation of forest structure and biomass *Int. J. Appl. Earth Obs. Geoinf.* **129** 103797
May P B, Dubayah R O, Bruening J M and Gaines G C 2025 GEDI-FIA Fusion: training lidar models to estimate forest attributes (https://doi.org/10.3334/ORNLDAAC/2417)
May P, McConville K S, Moisen G G, Bruening J and Dubayah R 2023 A spatially varying model for small area estimates of biomass density across the contiguous united states *Remote Sens. Environ.* **286** 113420
Meyer H and Pebesma E 2021 Predicting into unknown space? Estimating the area of applicability of spatial prediction models *Methods Ecol. Evol.* **12** 1620–33
Molina-Valero J A, Camarero J J, Alvarez-Gonzalez J G, Hevia A, Sanchez-Salguero R, Martin-Benito D and Pérez-Cruzado C 2021 Mature forests hold maximum live biomass stocks *Forest Ecol. Manage.* **480** 118635
Moore C R National old-growth amendment (available at: www.fs.usda.gov/inside-fs/leadership/national-old-growth-amendment)
Moore K D and Nelson M P 2023 The perilous and important art of definition: the case of the old-growth forest *Front. Ecol. Environ.* **21** 264–5
NASA JPL 2013 NASA shuttle radar topography mission global 3 arc second [data set] (https://doi.org/10.5067/MEaSUREs/SRTM/SRTMGL3.003)
Nelson P W 2012 Fire-adapted natural communities of the Ozark highlands at the time of european settlement and now *Proc. 4th Fire in Eastern oak Forests Conference* (*Springfield, MO, 17–19 May 2011) (Gen. Tech. Rep. NRS-P-102*), ed D C Dey, M C Stambaugh, S L Clark and C J Schweitzer (US Department of Agriculture, Forest Service, Northern Research Station)
Oliver C D, Larson B C and Oliver C D 1996 *Forest Stand Dynamics* (Wiley)
Omernik J M and Griffith G E 2014 Ecoregions of the conterminous United States: evolution of a hierarchical spatial framework *Environ. Manage.* **54** 1249–66
Owen R J, Duinker P N and Beckley T M 2009 Capturing old-growth values for use in forest decision-making *Environ. Manage.* **43** 237–48
Palik B J, D'Amato A W, Franklin J F and Johnson K N 2020 *Ecological Silviculture: Foundations and Applications* (Waveland Press)
Patterson P L *et al* 2019 Statistical properties of hybrid estimators proposed for GEDI-NASA's Global Ecosystem Dynamics Investigation *Environ. Res. Lett.* **14** 065007
Pelz K A, Hayward G, Gray A N, Berryman E M, Woodall C W, Nathanson A and Morgan N A 2023 Quantifying old-growth forest of United States Forest Service public lands *Forest Ecol. Manage.* **549** 121437
Pesklevits A, Duinker P N and Bush P G 2011 Old-growth forests: anatomy of a wicked problem *Forests* **2** 343–56
Ploton P *et al* 2020 Spatial validation reveals poor predictive performance of large-scale ecological mapping models *Nat. Commun.* **11** 4540
Roos C I *et al* 2021 Native American fire management at an ancient wildland–urban interface in the southwest United States *Proc. Natl Acad. Sci.* **118** e2018733118
Spies T A 2004 Ecological concepts and diversity of old-growth forests *J. Forestry* **102** 14–20
Spies T A and Franklin J F 1996 The diversity and maintenance of old-growth forests *Biodiversity in Managed Landscapes: Theory and Practice* (Oxford University Press) pp 296–314
Taylor A H, Trouet V, Skinner C N and Stephens S 2016 Socioecological transitions trigger fire regime shifts and modulate fire–climate interactions in the Sierra Nevada, USA, 1600–2015 CE *Proc. Natl Acad. Sci.* **113** 13684–9
Trouvé R, Jiang R, Baker P J, Kasel S and Nitschke C R 2023 Identifying old-growth forests in complex landscapes: a new lidar-based estimation framework and conservation implications *Remote Sens.* **16** 147
Tulowiecki S J 2024 Compiling historical descriptions of past indigenous cultural burning: a dataset for the eastern United States *Int. J. Wildland Fire* **33** WF24029
Tyrrell L E 1998 *Information About old Growth for Selected Forest Type Groups in the Eastern United States* vol 197 (US Department of Agriculture, Forest Service, North Central Forest)
Tyukavina A *et al* 2022 Global trends of forest loss due to fire from 2001 to 2019 *Front. Remote Sens.* **3** 825190
Various authors 1993 Interim old growth definitions for douglas-fir, grand fir/white fir, interior douglas-fir, lodgepole pine, pacific silver fir, ponderosa pine, port orford-cedar and tanoak, subalpine fir, and western hemlock series (US Department of Agriculture, Forest Service) vol 124
White C A, Perrakis D D B, Kafka V G and Ennis T 2011 Burning at the edge: integrating biophysical and eco-cultural fire processes in Canada's parks and protected areas *Fire Ecol.* **7** 74–106
Wirth C, Gleixner G and Heimann M 2009 *Old-Growth Forests: Function, Fate and Value–an Overview* (Springer)
Wirth C, Messier C, Bergeron Y, Frank D and Fankhänel A 2009 *Old-Growth Forest Definitions: a Pragmatic View* (Springer)
Woodall C W, Kamoske A G, Hayward G D, Schuler T M, Hiemstra C A, Palmer M and Gray A N 2023 Classifying mature federal forests in the United States: the forest inventory growth stage system *Forest Ecol. Manage.* **546** 121361